Synthesis and Spectral Characterization of Bimetallic Metallomacrocyclic Structures $[M^{II}_2$-μ^2-bis-{(κ^2S,S-$S_2CN(R)C_6H_4)_2O$}] (M= Ni/Zn/Cd): Density Functional Theory and Host-Guest Reactivity Studies

Rahul Kadu, Vineeta Pillai, Amrit V. and Vinay K. Singh*

Department of Chemistry, Faculty of Science, The M. S. University of Baroda,

Vadodara-390 002, India;

*Email: vks.msu@gmail.com; vinay.singh-chem@msubaroda.ac.in

Electronic Supplimentary Information

Contents

I. Spectral Characterization

1. Mass Spectra:

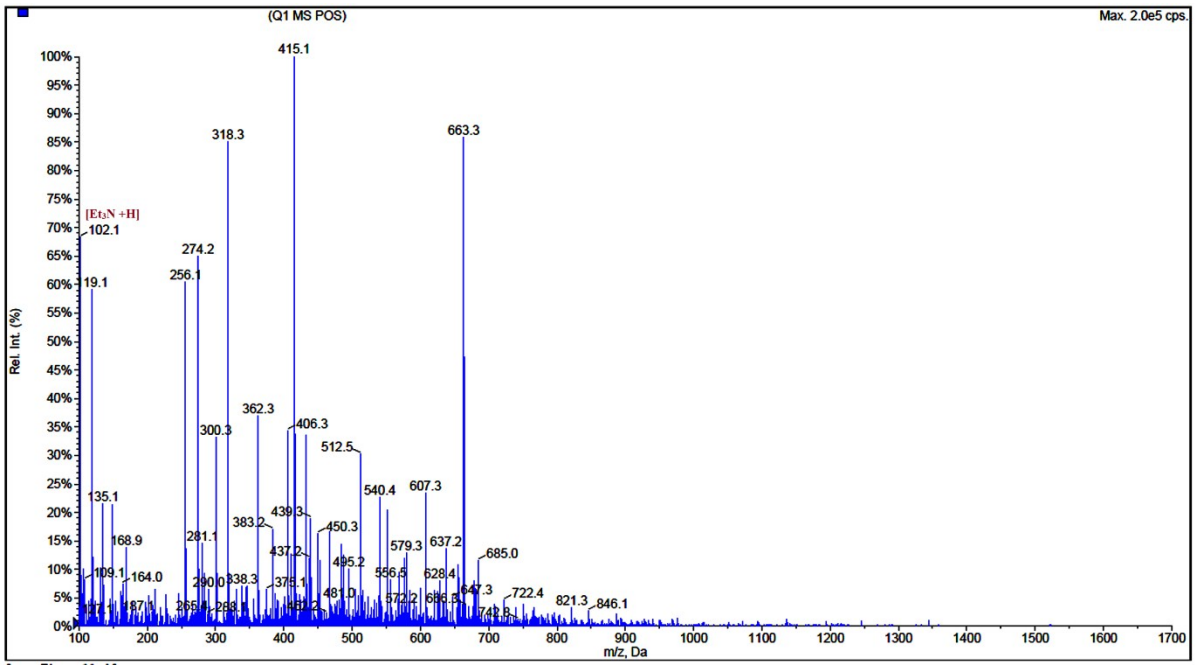

Fig. S1 Mass spectrum (positive ion mode) of complex **1**.

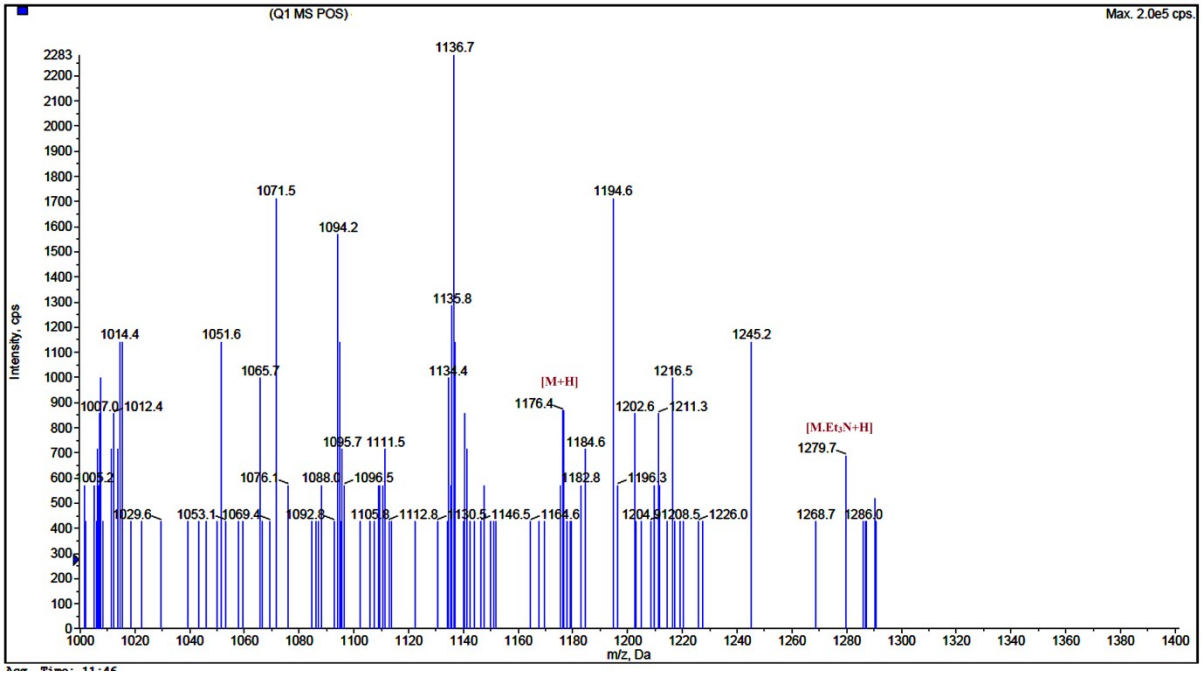

Fig. S2 Mass spectrum (positive ion mode) of complex **1**.

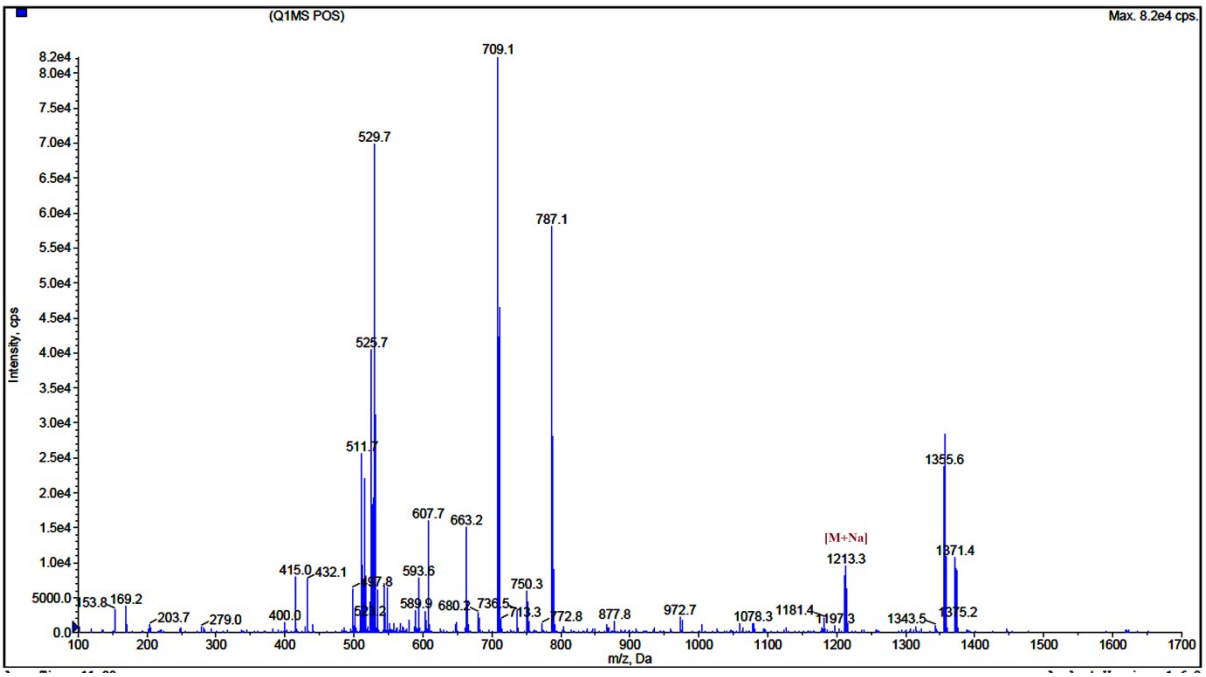

Fig. S3 Mass spectrum (positive ion mode) of complex **2**.

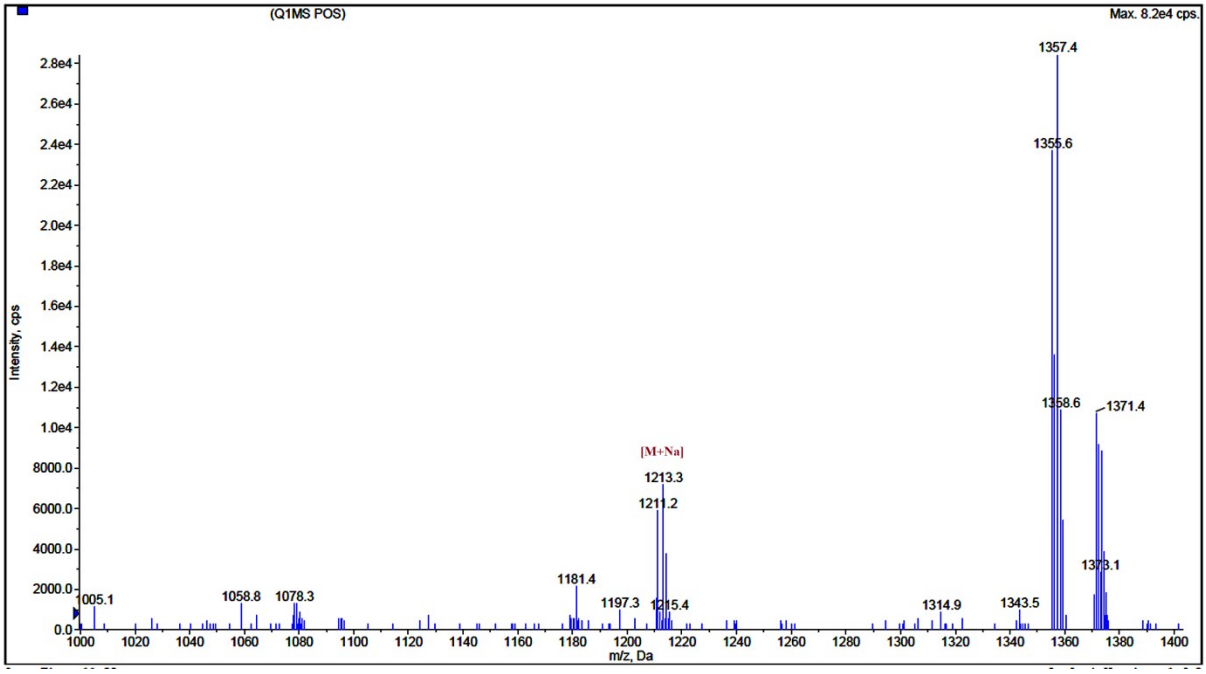

Fig. S4 Mass spectrum (positive ion mode) of complex **2**.

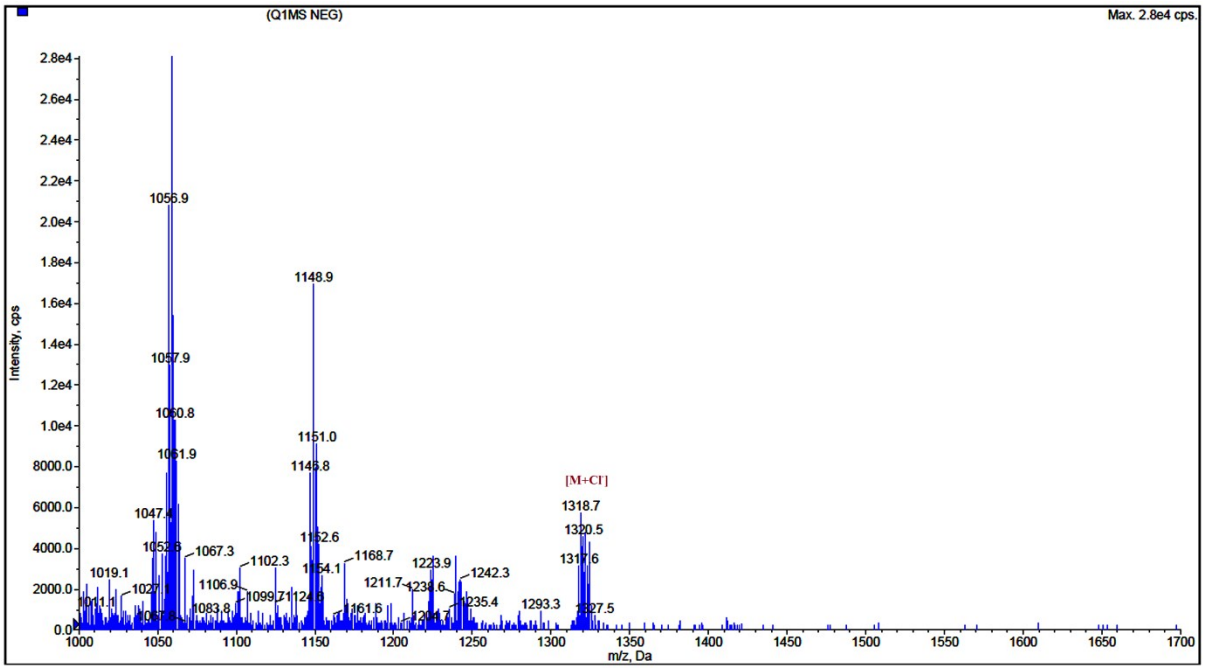

Fig. S5 Mass spectrum (negative ion mode) of complex **3**.

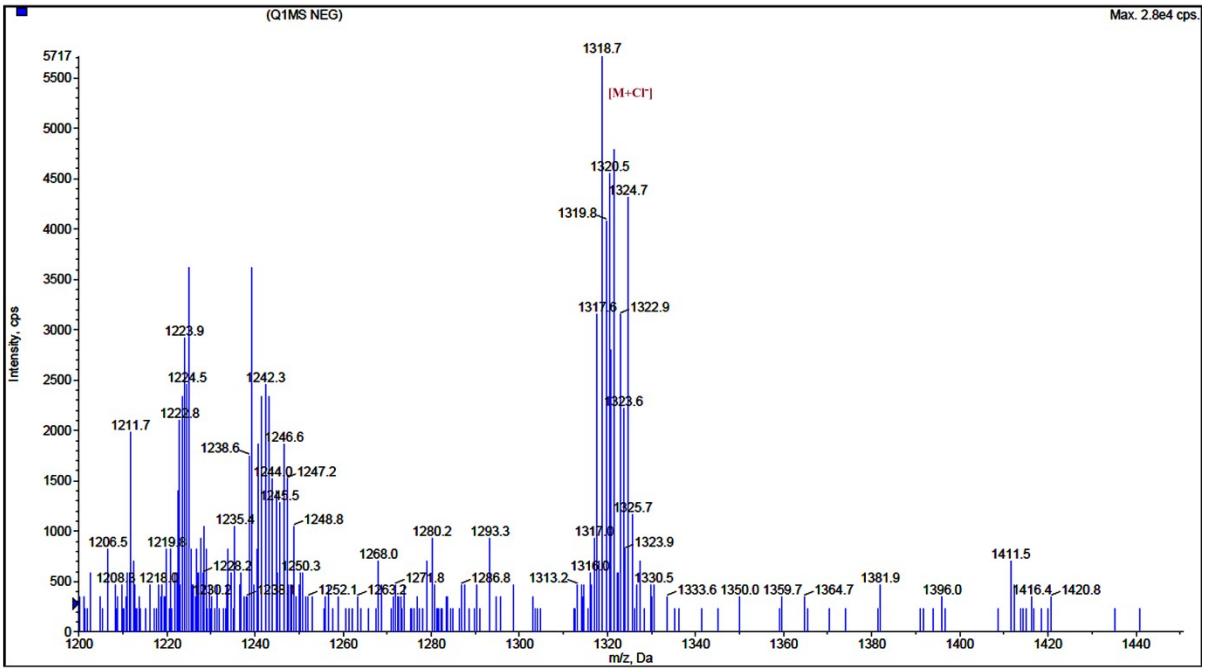

Fig.S6 Mass spectrum (negative ion mode) of complex **3**.

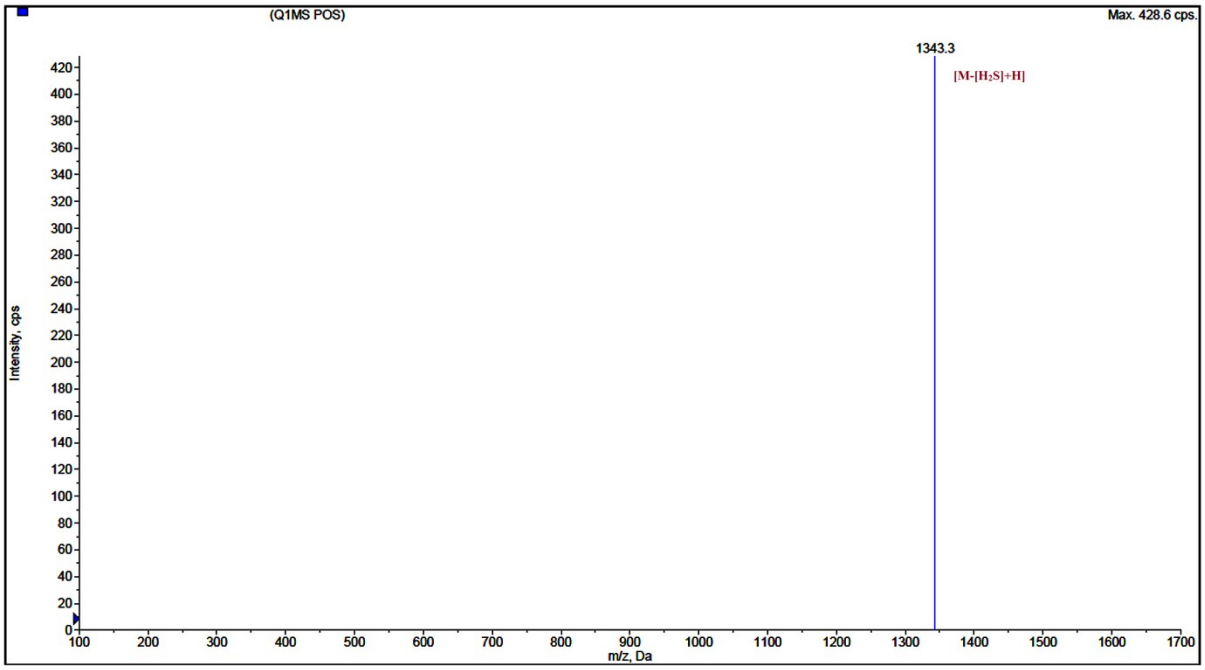

Fig.S7 Mass spectrum (positive ion mode) of complex **4**.

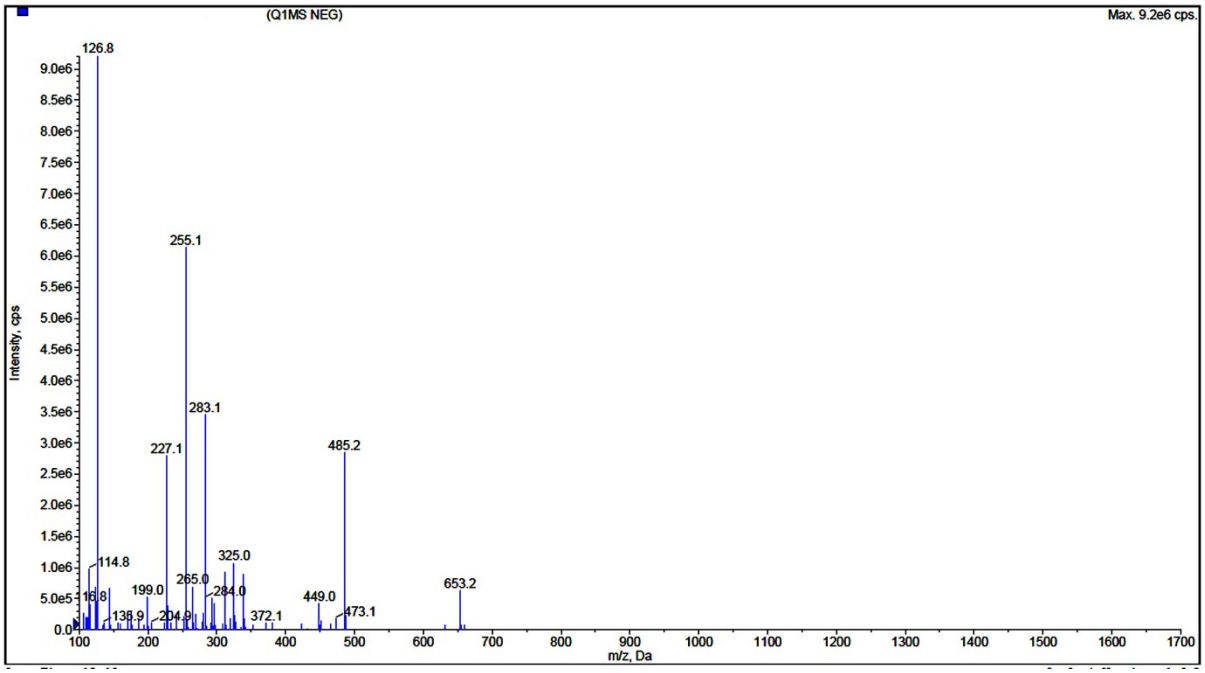

Fig. S8 Mass spectrum (negative ion mode) of complex **4**.

Table S1 Mass Analysis of binuclear M^{II}dithiocarbamate complexes (**1-4**)

m/z	Possible fragments
Complex 1 (1175.99)	
1279.7	[M.Et_3N+H]
1194.6	[M+19] (19: NH_4/H_3O)
1176.4	[M+H]
663.3	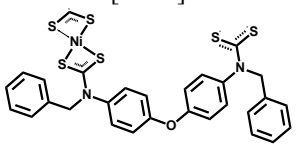

512.5	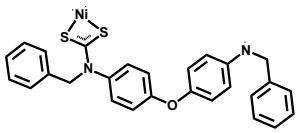
391.91	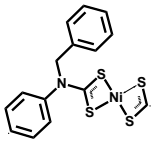
415.91	[391.91 + 23]
102.1	[Et_3N+H]
	Complex 2 (1187.98)
1356.58	[M + diphenylether]
1213.3	[M+Na]
709.1	[699.05 +3Li+H]
699.05	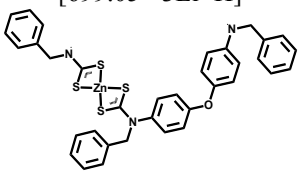
593.6	Symmetrical cleavage
102.1	No peak for Et_3N
	Complex 3 (1287.93) (negative ion mode)
1320.5	1285.93 + Cl^-
1148.9	[1058+benz+H^-]
1022.14	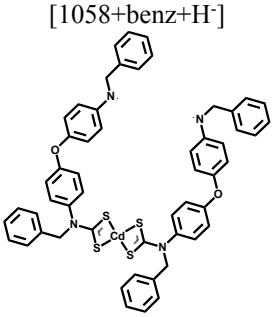
1058	[1022.14 + Cl^-] OR [M-(Cd+2CS_2)+Cl^-]
	Complex 4 (1376.06)
1343.3	[(M-S) + H]
653.2	[630.09 + 23]
630.09	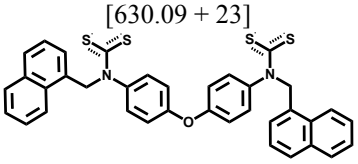
485.2	[478.20 + 2Li+ H^-]
478.20	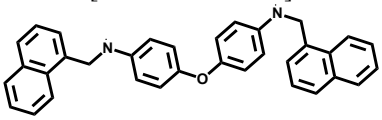
255.1	[254.02 + H^-]
254.02	[231.02 + 23]
231.02	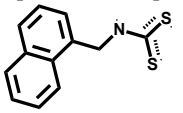
126.8	

2. IR spectra

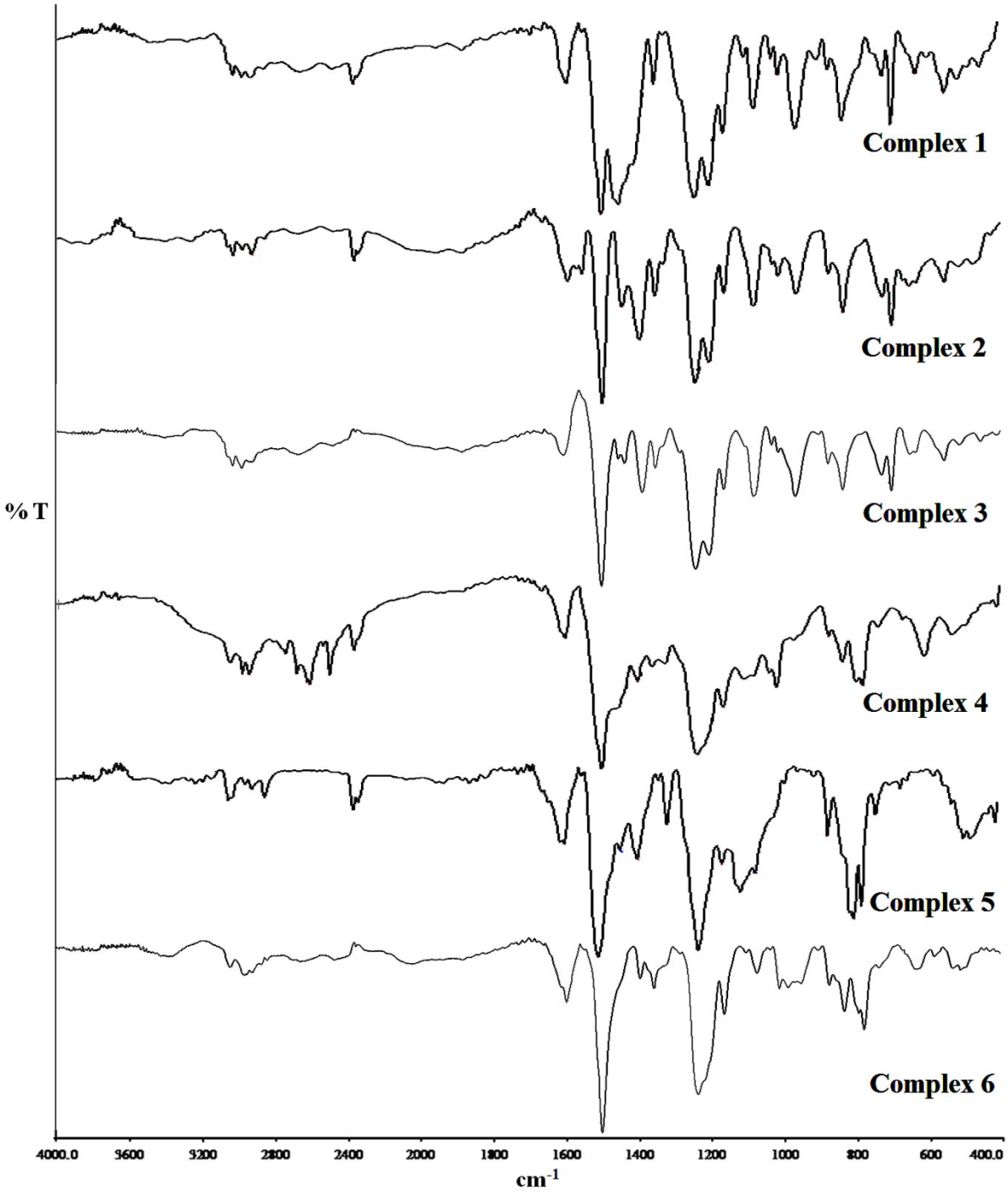

Fig. S9 IR spectra of complex **1-6**.

3. NMR spectra

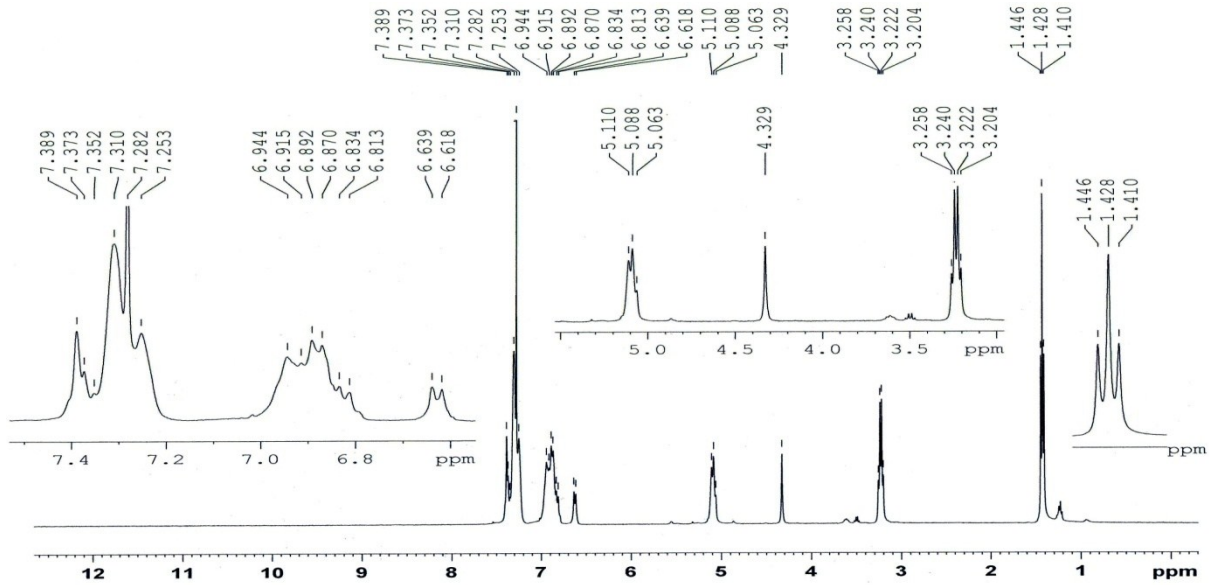

Fig. S10 ^{1}H NMR spectrum of complex **1**.

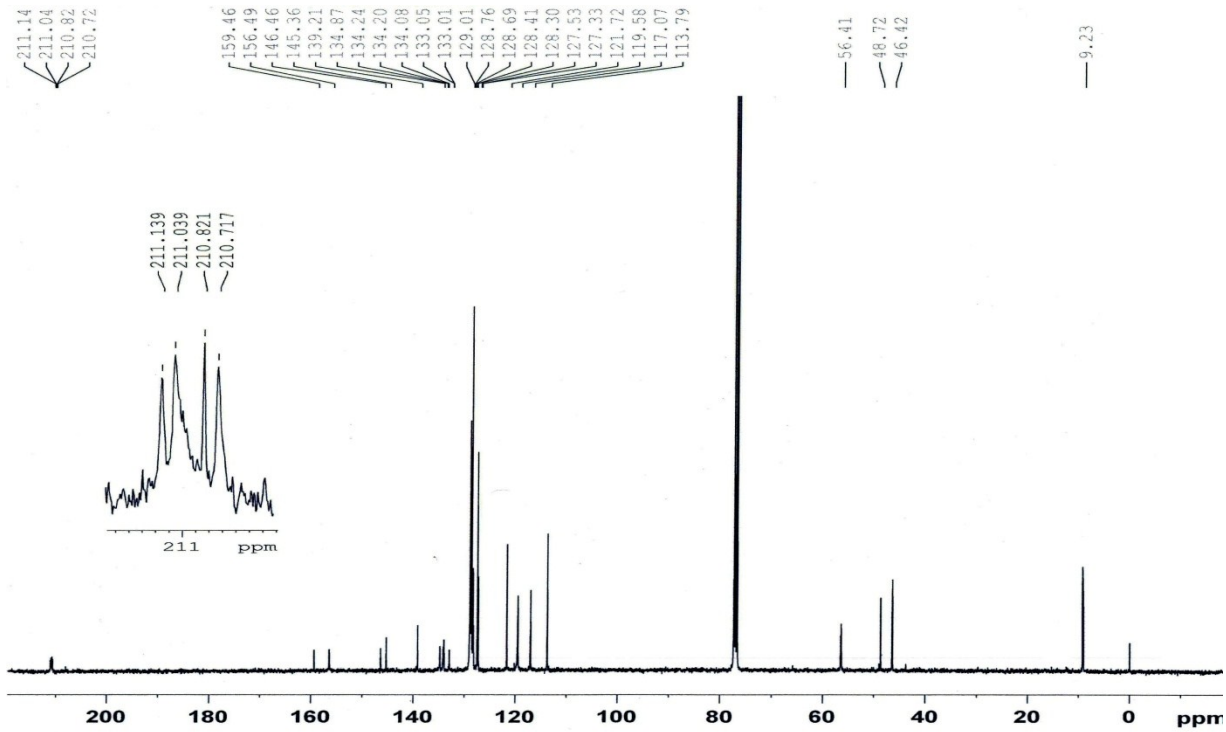

Fig S11 ^{13}C NMR spectrum of complex **1**.

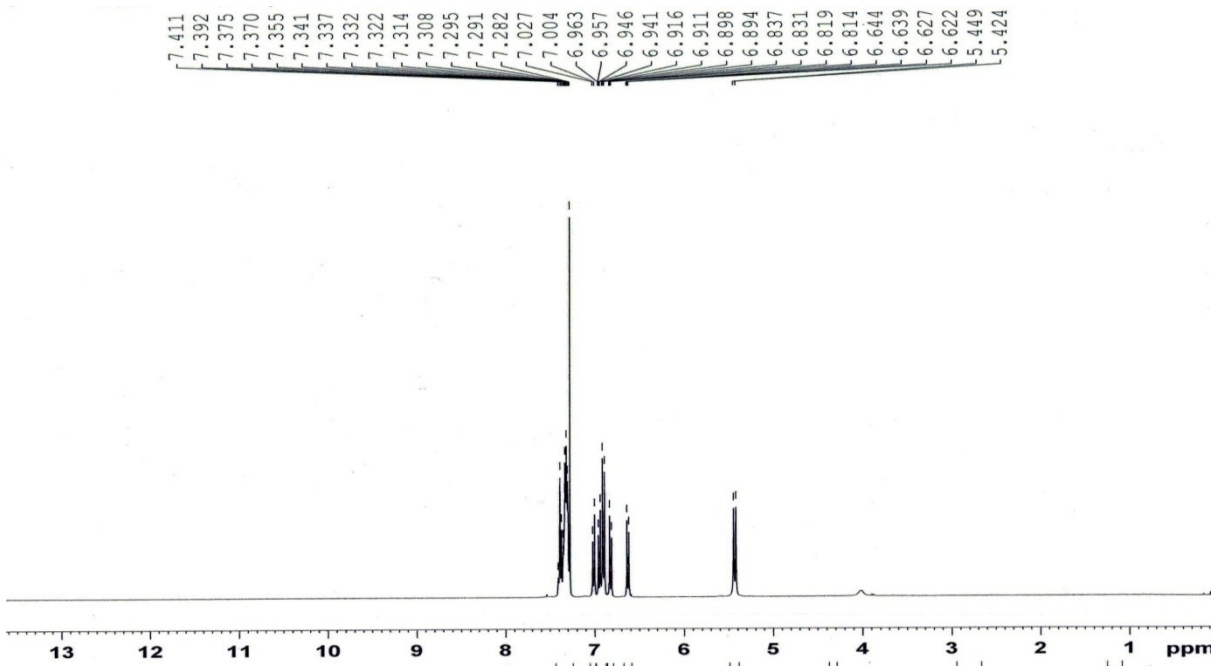

Fig. S12 ^{1}H NMR spectrum of complex **2**.

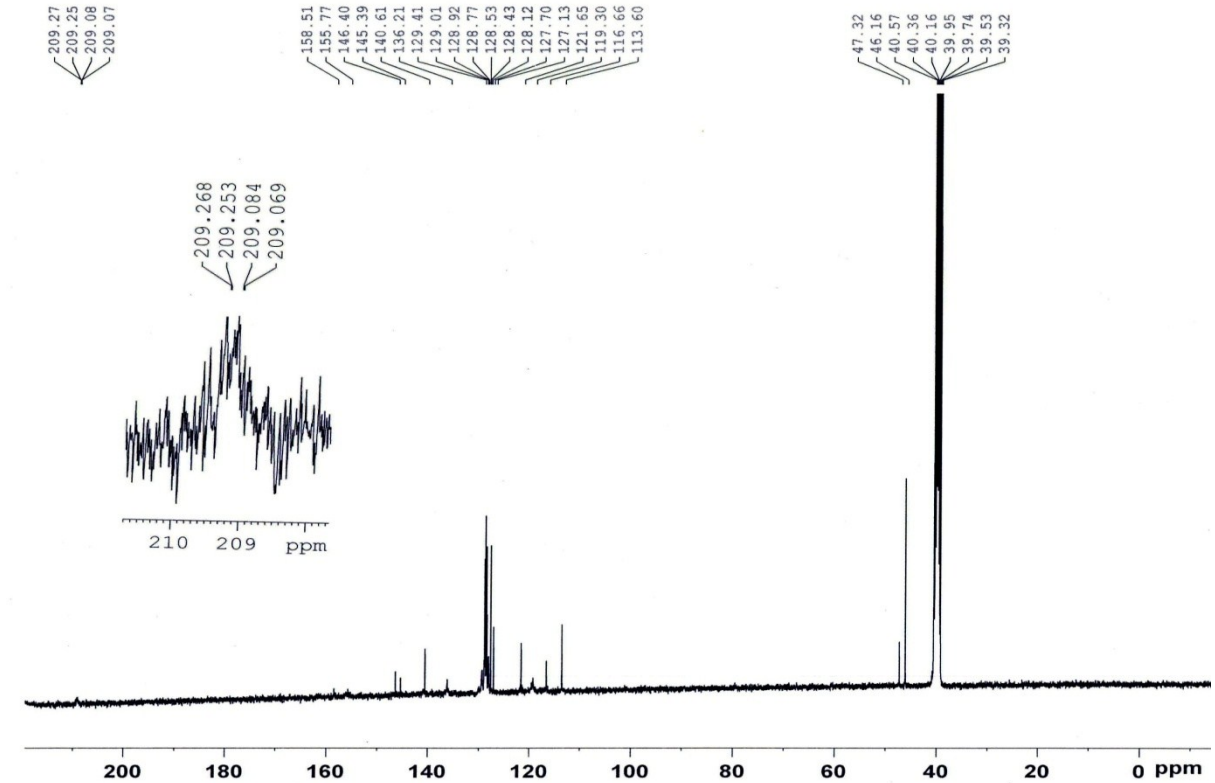

Fig. S13 ^{13}C NMR spectrum of complex **2**.

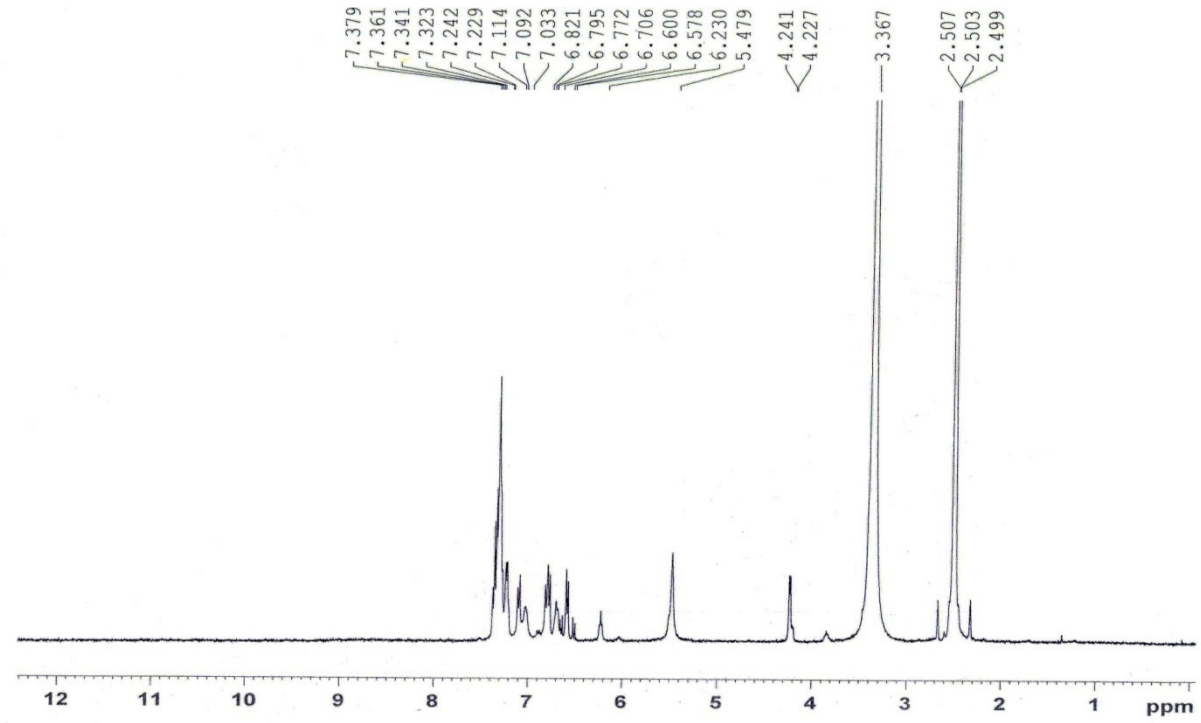

Fig. S14 ^{1}H NMR spectrum of complex **3**.

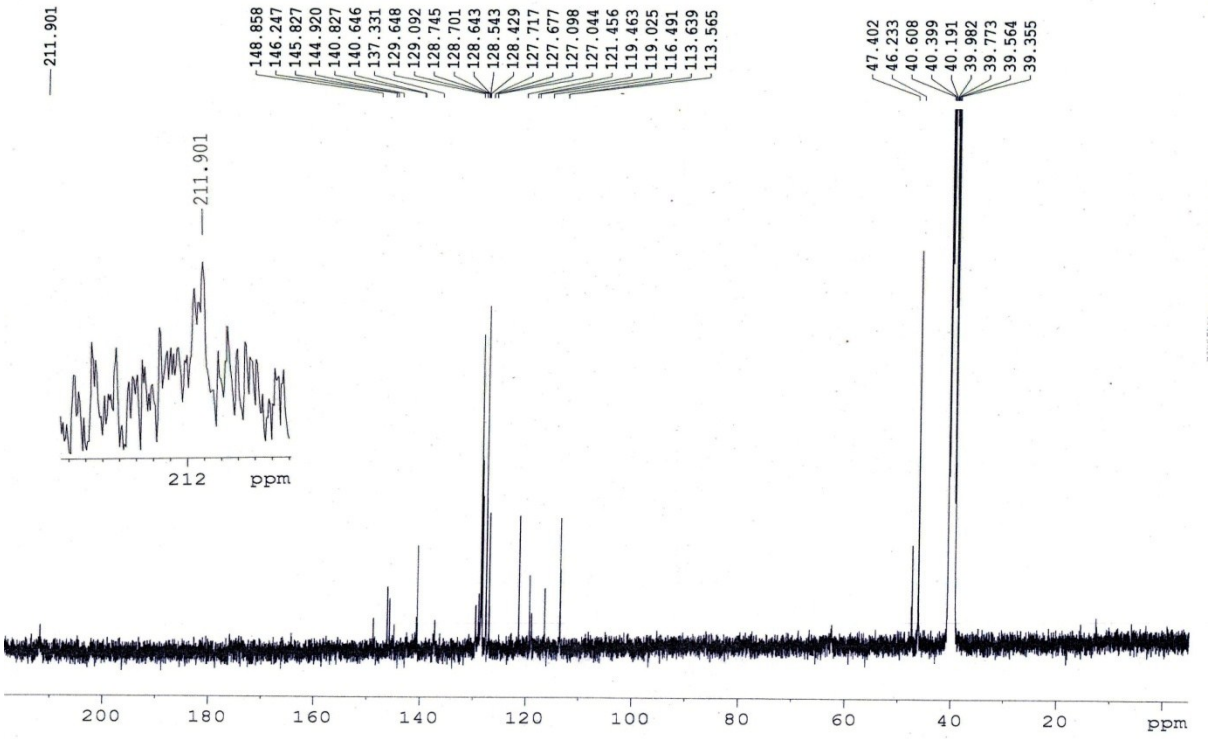

Fig. S15 ^{13}C NMR spectrum of complex **3**.

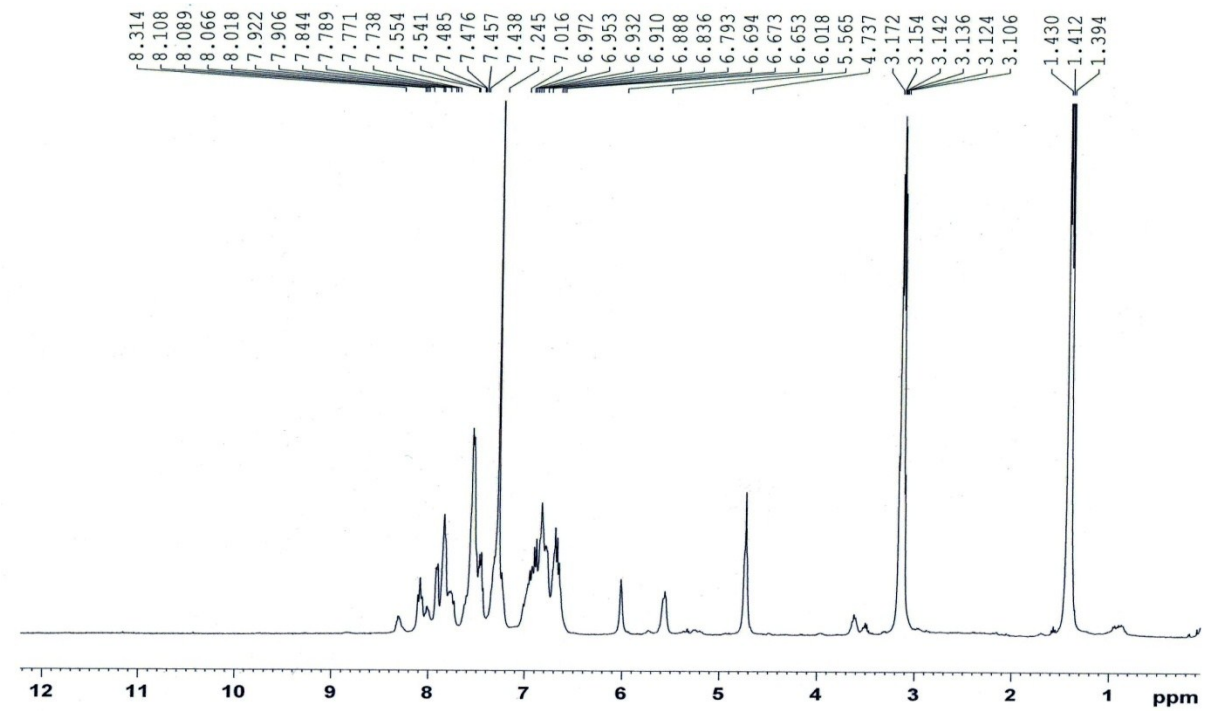

Fig. S16 ^{1}H NMR spectrum of complex **4**.

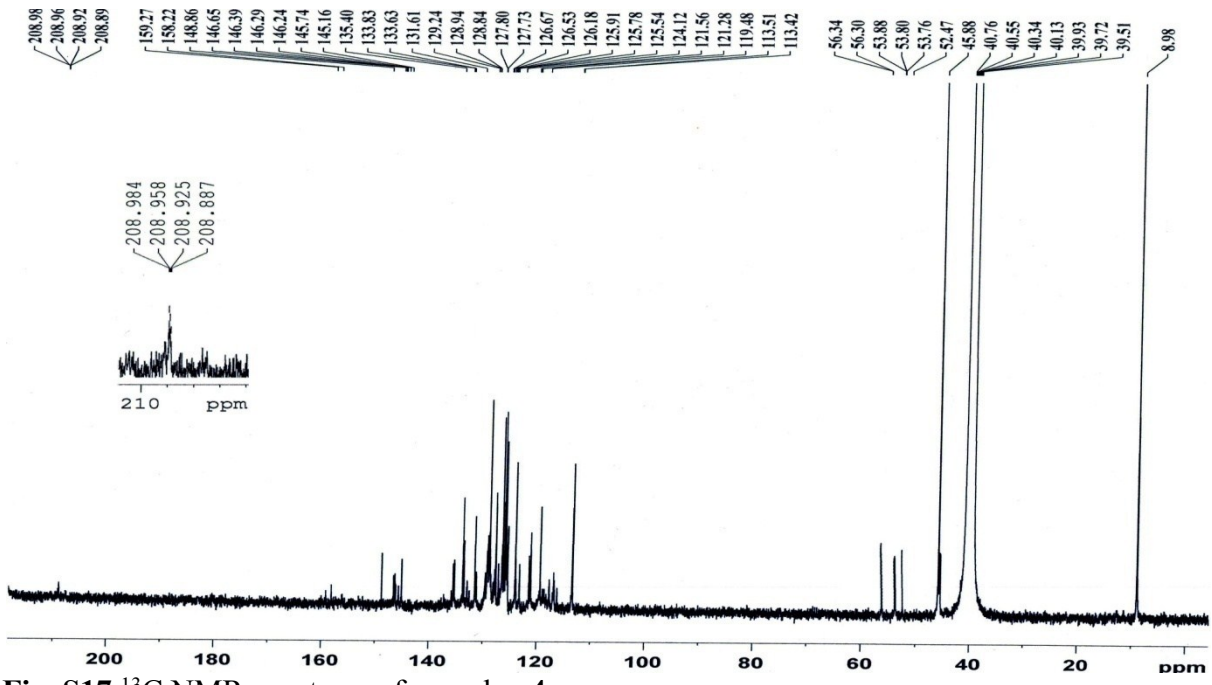

Fig. S17 ^{13}C NMR spectrum of complex **4**.

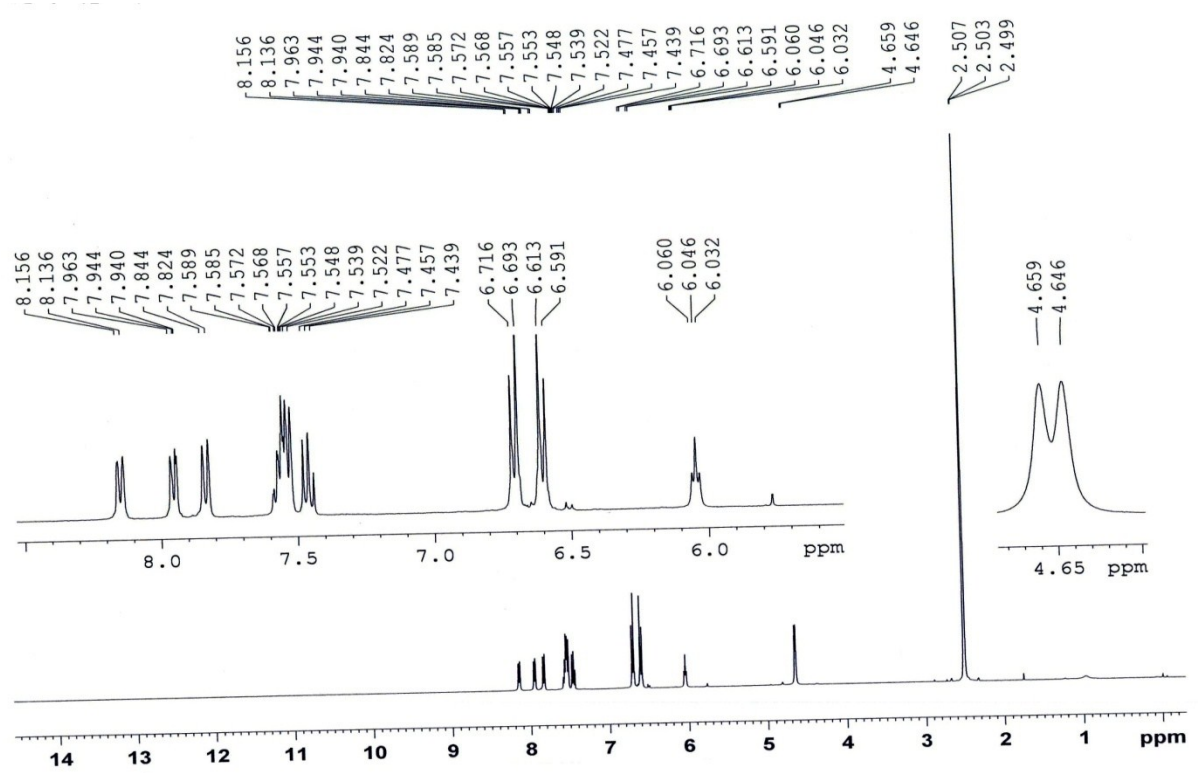

Fig. S18 ^{1}H NMR spectrum of complex **5**.

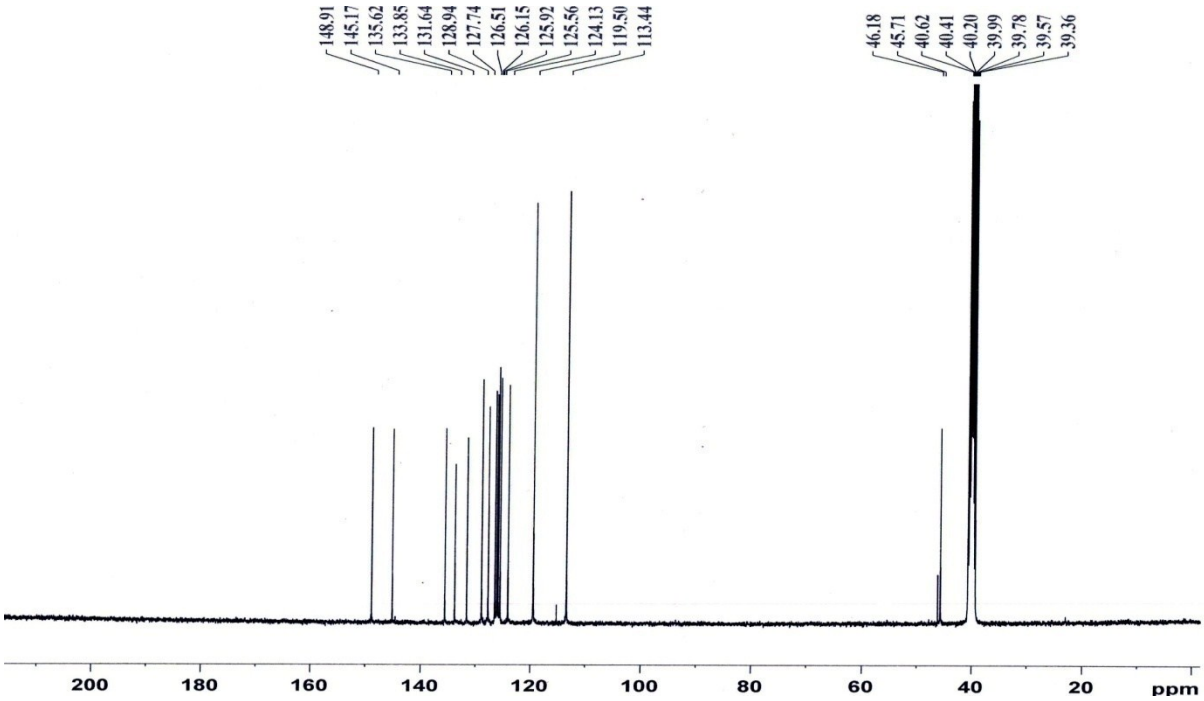

Fig. S19 ^{13}C NMR spectrum of complex **5**.

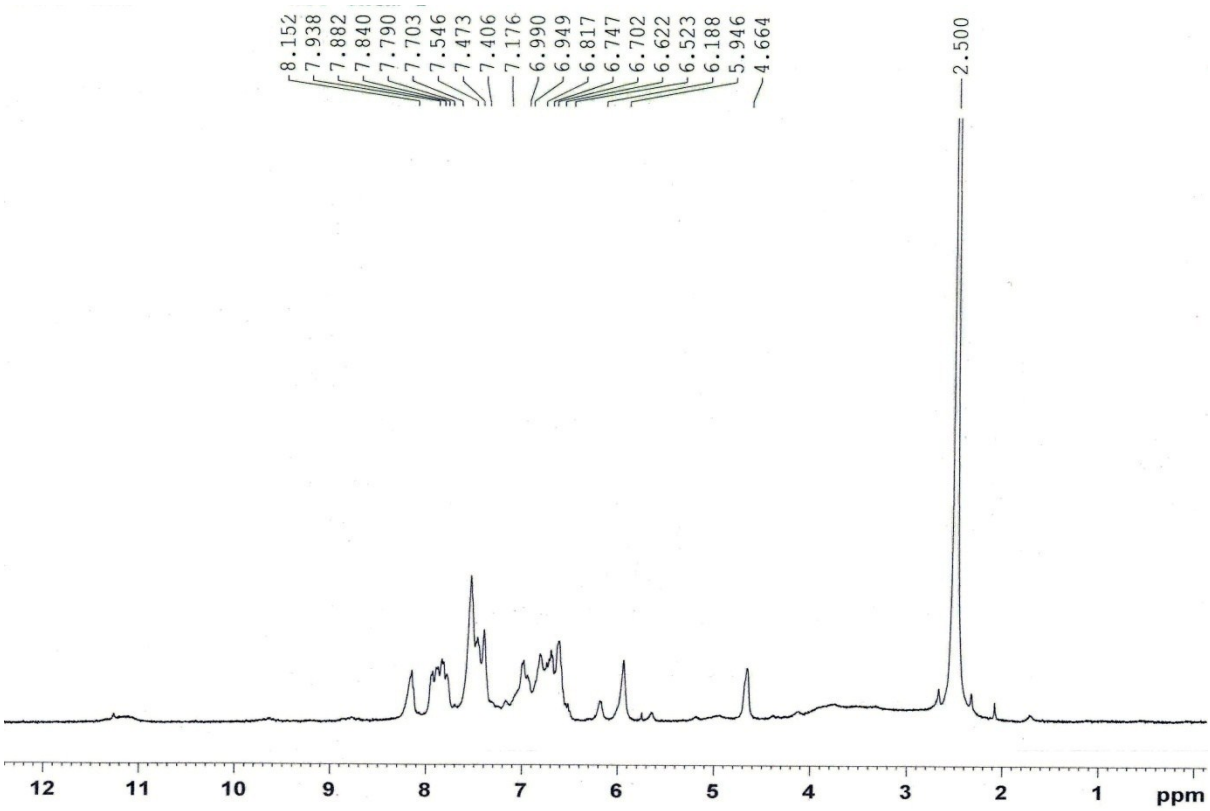

Fig. S20 ^{1}H NMR spectrum of complex **6**.

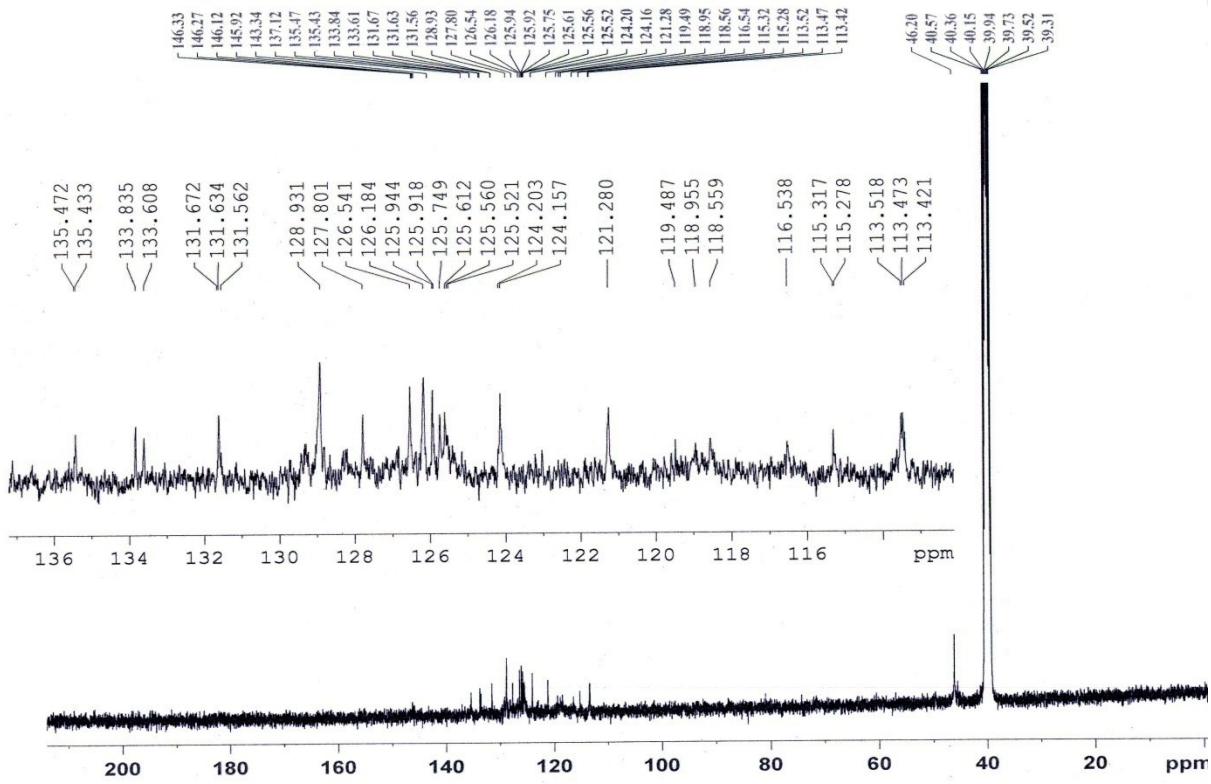

Fig. S21 ^{13}C NMR spectrum of complex **6**.

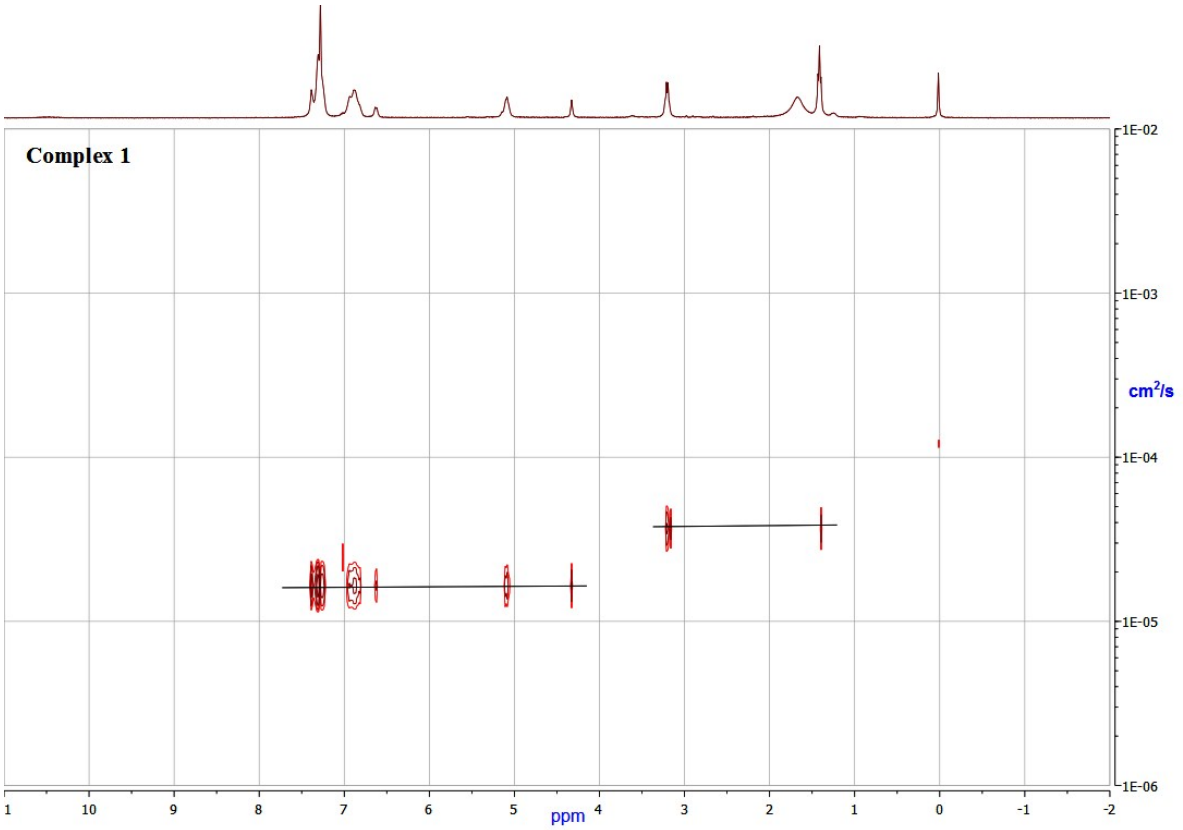

Fig. S22 ^{1}H DOSY NMR spectrum of complex **1**.

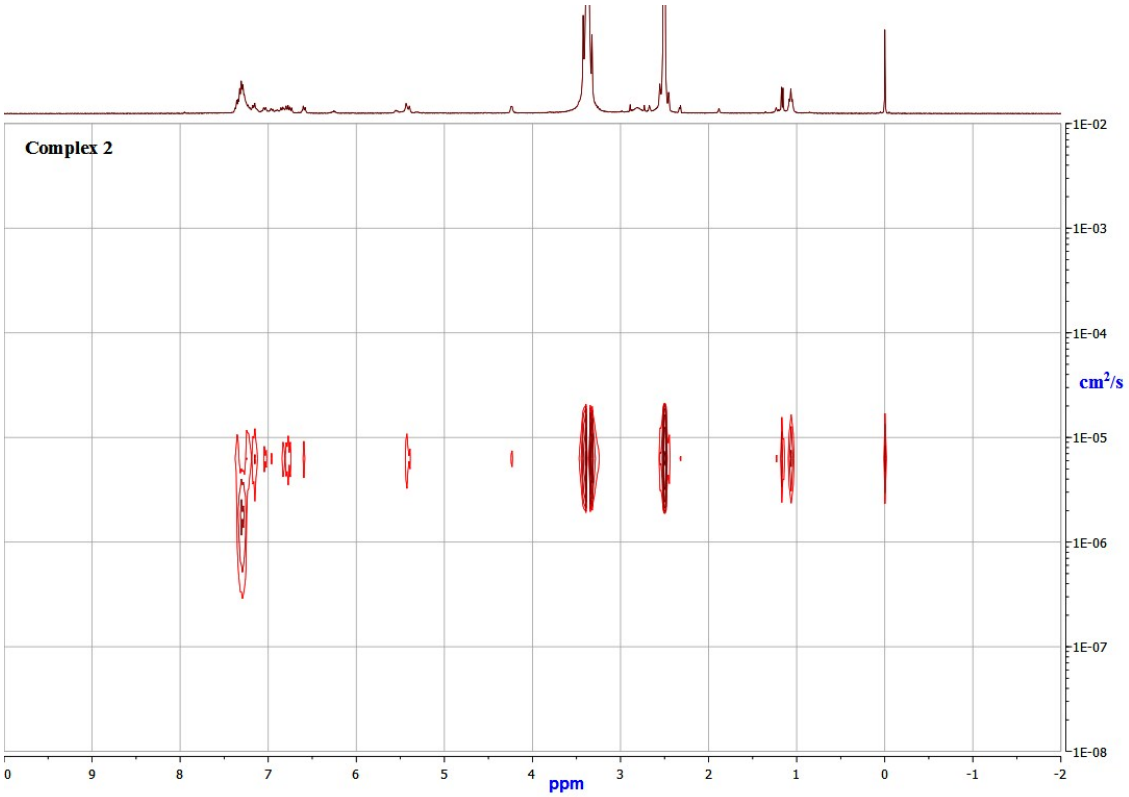

Fig. S23 ^{1}H DOSY NMR spectrum of complex **2**.

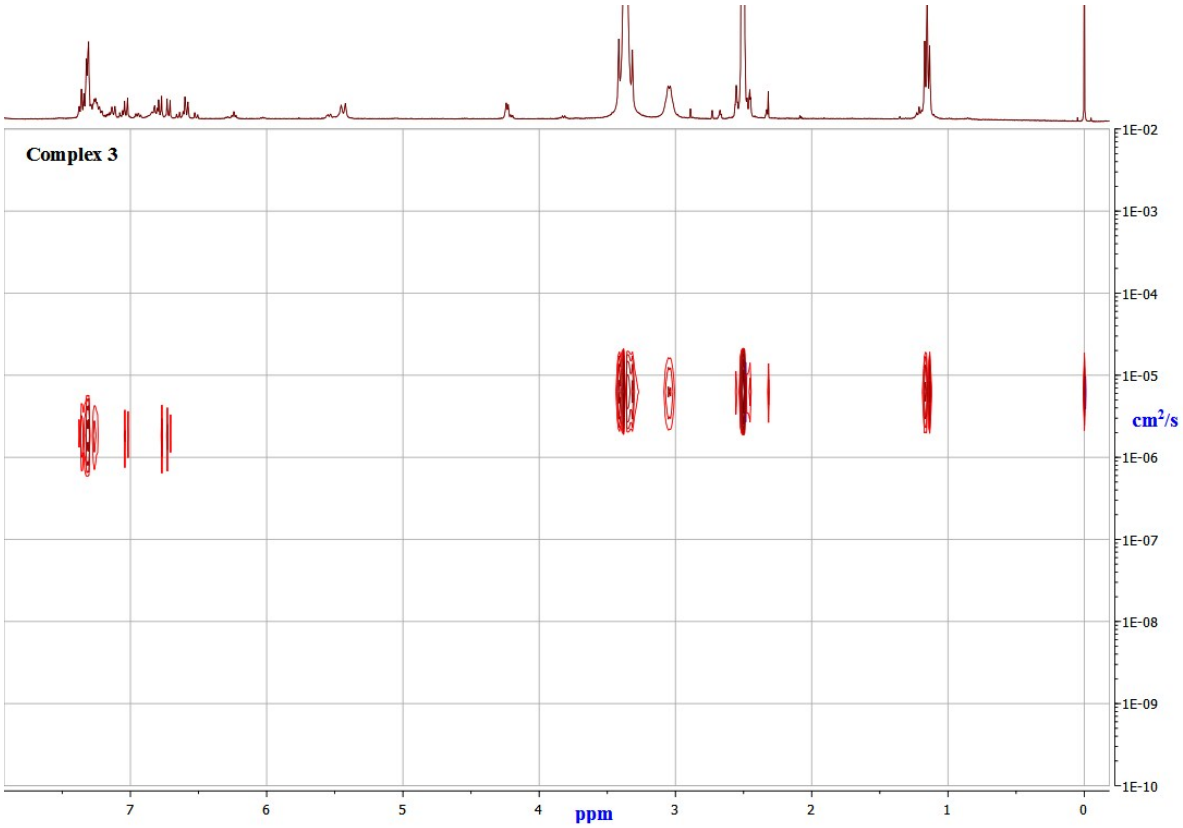

Fig. S24 ^{1}H DOSY NMR spectrum of complex **3**.

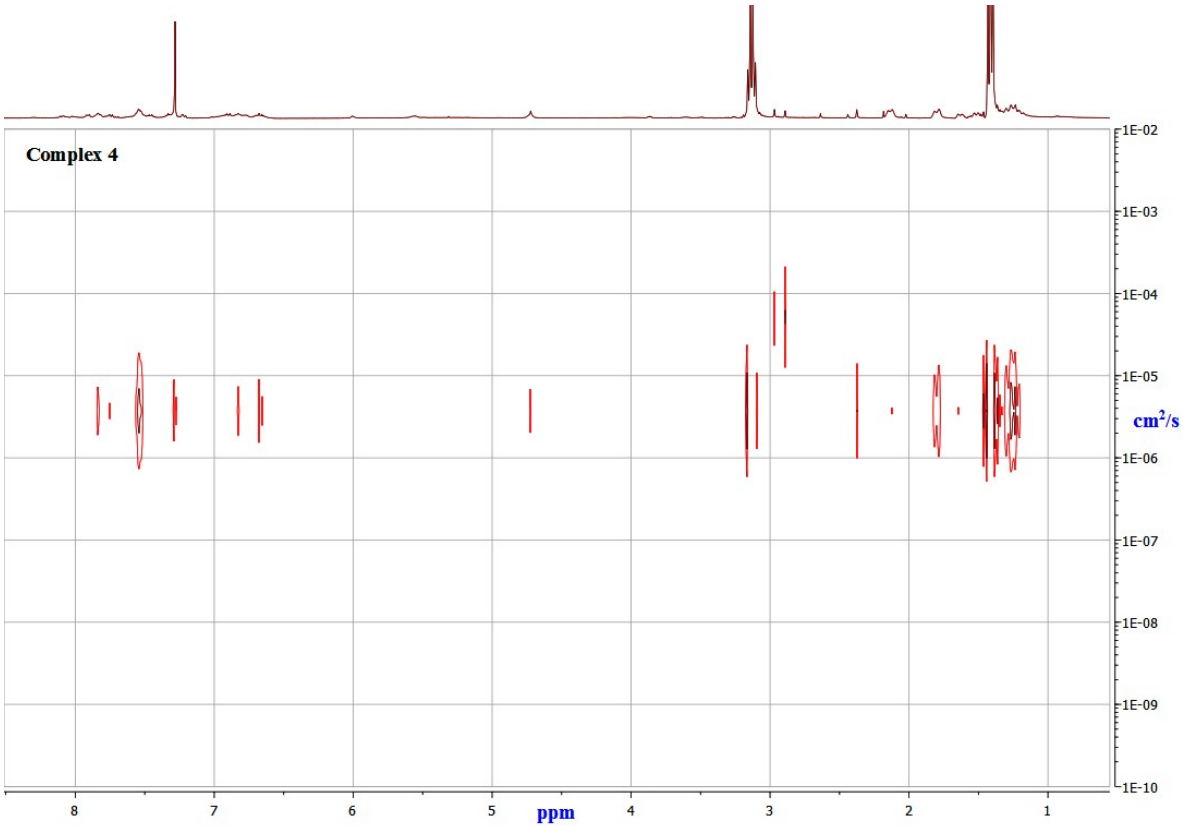

Fig. S25 ^{1}H DOSY NMR spectrum of complex **4**.

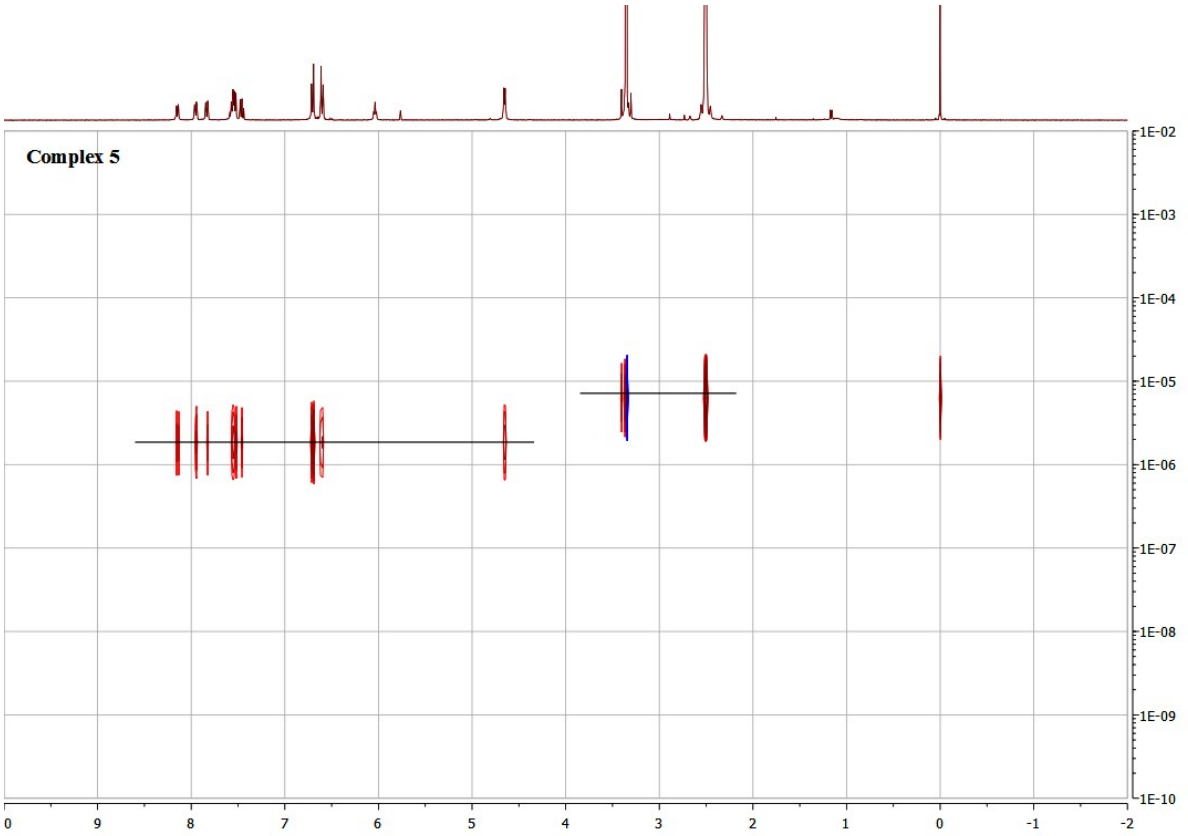

Fig. S26 ^{1}H DOSY NMR spectrum of complex **5**.

II. Optical Properties

1. UV-Visible Absorption

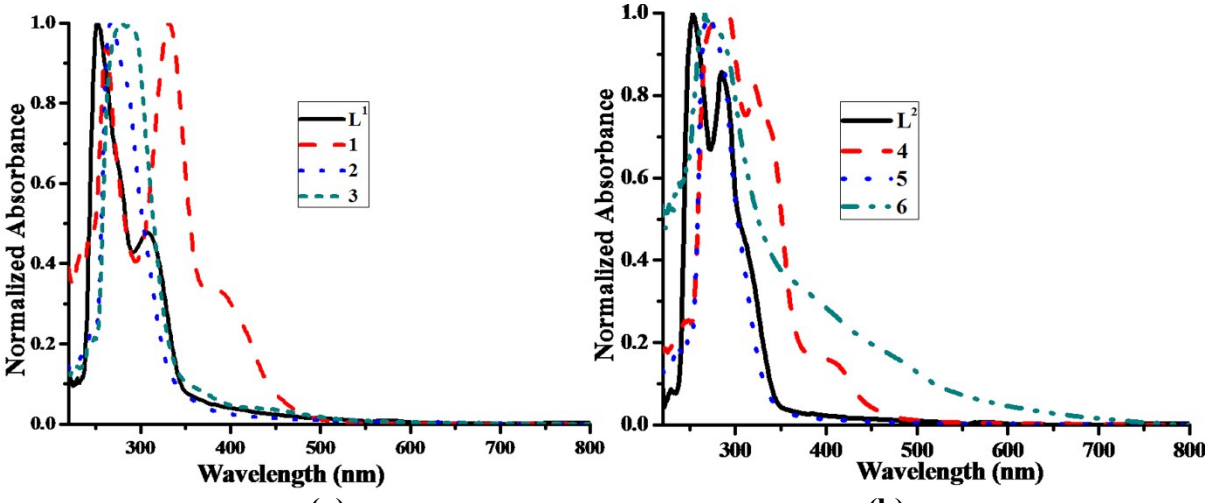

Fig. S27 UV–visible absorption spectra of compounds $\mathbf{L^1}$, $\mathbf{L^2}$ and **1-6** in 10^{-5} M DMSO solution.

2. Uv-visible transmittance (Optical Band gap)

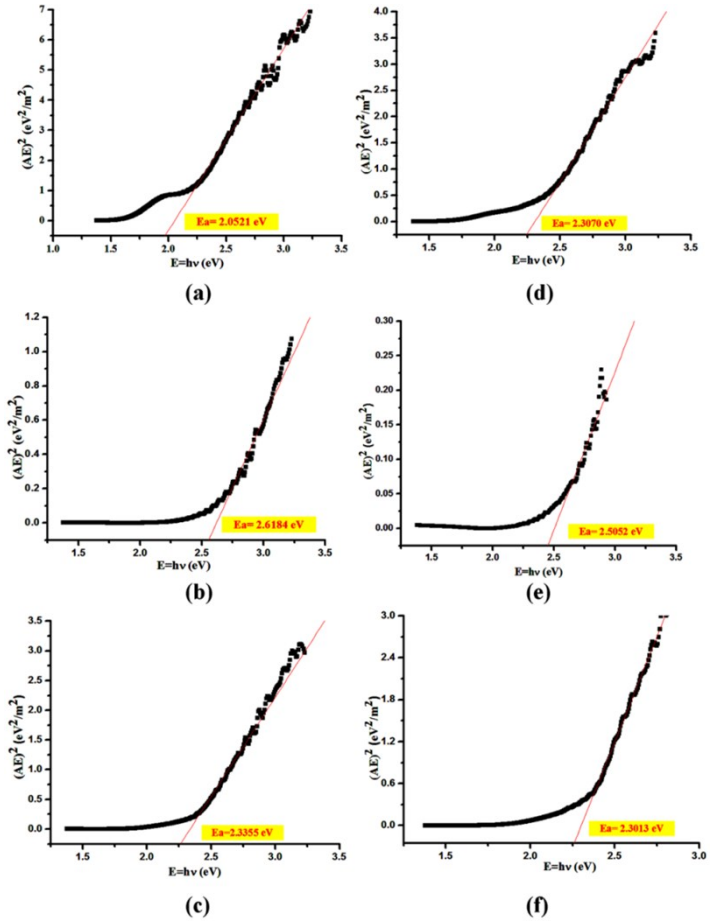

Fig. S28 Tauc plot illustrating the optical band gap for **1-6** by UV–visible transmittance study.

Optical Properties

UV-visible absorption, emission and transmittance

The UV-visible absorption and emission spectra of ligand precursors **L[1]**, **L[2]** and binuclear metallomacrocyclic dithiocarbamate complexes **1-6** were measured at room temperature from 10^{-5} M DMSO solution samples. The UV-visible absorption of the investigated compounds is provided above (Fig. S27), while the emission spectra is provided in the manuscript. The pertinent results are summarized in Table S2.

Table S2 UV–visible absorption, emission and optical band gap data for ligand precursors [a] **L[1], L[2]** and binuclear metallomacrocyclic dithiocarbamate complexes **1-6**.

Entry	UV-Visible Absorption Spectral data λ_{max} nm (ε, L mol^{-1} cm^{-1})	Emission Spectral data λ_{em} nm (Intensity)	λ_{ex} (nm)	Band Gap Ea (eV)
L^1	253 (38616) π→π* (phenyl) 307 (17366) n→π* (amine)	360 (36) π*→n (dtc)	307	2.1677
L^2	253 (35066) π→π* (phenyl) 285 (29934) π→π* (amine)	346 (7) π*→π (phenyl) 497 (8) π*→π (phenyl)	284	2.2897
1	261 (56324) π→π* (phenyl) 332 (57565) n→π* (N–C=S) 388sh (19509) charge transfer	308 (193) π*→π (phenyl) 372(1000) π*→π (phenyl) 536(321) π*→π (phenyl)	261	2.0521
2	267(58322) π→π* (phenyl)	328(36) π*→π (phenyl) 371(211) π*→π (phenyl)	267	2.6184
3	282 (52417) π→π* (phenyl) 438 (21498) charge transfer	416 (105) π*→π (phenyl) 437 (114) br, π*→π (phenyl)	282	2.3355

4	286 (51860) π→π* (phenyl) 326 (43096) n→π* (N–C=S) 409sh (8102) charge transfer	374 (165) π*→ n (dtc) 533 (517) π*→ n (dtc) 586 (355) π*→ n (dtc) 640 (269) π*→ n (overtone)	326	2.3070
5	271 (45387) π→π* (phenyl)	371 (697) π*→π (phenyl)	271	2.5052
6	265(15361) π→π* (phenyl) 478(31961) charge transfer	330 (775) π*→π (phenyl)	265	2.3013

a: For comparison, UV-visible absorption, emission and transmittance data retrieved from references 18a, 21 of the ms.

The fluorescence study evidently depicted the enhancement in fluorescence property of binuclear complexes **1-6**, compared to their respective ligand precursors $\mathbf{L^1}$ and $\mathbf{L^2}$. This can be expected due to an efficient delocalization of π-electrons and conformational rigidity acquire by the macrocyclic molecular framework, reducing the nonradiative decay. All the complexes **1-6** exhibit maximum fluorescence emissions at 372, 371, 437, 533, 371 and 330 nm upon excitation at 261, 267, 282, 326, 271 and 265 nm with concomitant Stokes shifts of 111, 96, 155, 207, 100 ≈ 65 nm, respectively. (Manuscript, Fig. 3) Notably, among **1-6**, complex **1** bearing Ni^{II} centre exhibit the maximum fluorescence property which may be attributed to the reduction of photoinduced electron transfer process on complex formation. The emission spectra of majority of the complexes displayed similar patterns, i.e. two or more kinds of fluorescence emission bands are appearing by the excitation of single absorption bands (in any case, shoulder is appearing). Such a trend of fluorescence spectra and concomitant bathochromic shifts of intramolecular charge-transfer emissions is consistent with previous reports on transition metal dithiocarbamate complexes.

Furthermore, all the complexes **1–6** were investigated for their potential optical behaviour towards wide band-gap semiconducting nature using UV–visible transmittance measurements. The values of optical energy band gaps and their nature were derived from electronic excitation from the valence band to conduction band as described elsewhere. The optical absorption coefficients, α; were obtained from the transmittance spectrum of complexes **1–6** using the formula: $\alpha = \frac{1}{d} ln[\frac{1}{T}]$, where, d is the thickness of the samples and T is the transmittance. The relation between the absorption coefficients (α) and the incident photon energy (hν) can be determined using the well known Davis and Mott equation,[1] $\alpha h\nu = [D(h\nu - Eg)]^{\gamma}$ where, constant D is the edge width parameter. The exponent γ depends on the type of transition occur in the material. In order to determine optical band gap energies (*Eg*) for binuclear metallomacrocyclic dithiocarbamate complexes **1-6**, we have applied the models for both direct and indirect transitions. For this, the $(\alpha h\nu)^2$ (direct transition) and $(\alpha h\nu)^{1/2}$ (indirect transitions) versus hν were plotted for each compound. The values of *Eg* obtained for an entire group of compounds **1-6** by extrapolating the linear part of the Tauc plot[2] (with c = 1/2) (Fig. S28) suggest the absorption in these samples corresponds to a direct energy gap. The band gap energy for all the complexes falls in 2.1-2.6 eV range and exhibits a feature of direct band gap semiconductor. Expectedly the *Eg* for all the complexes (except **1**) are higher than their corresponding diamine precursors as polyamines are well known conducting materials with lower band gap energies.

III. Thermogravimetric Study

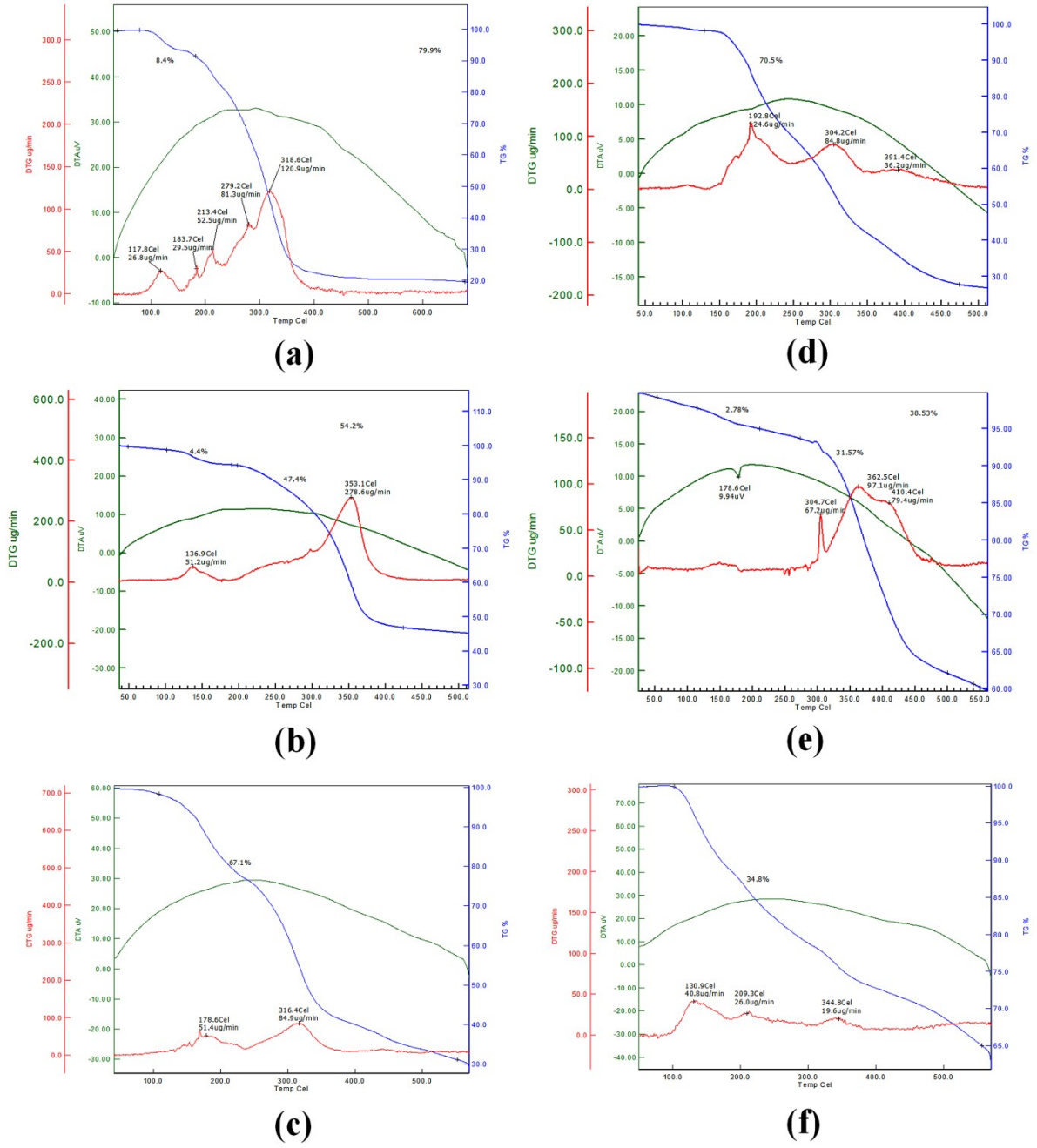

Fig. S29 TGA/DTA plots, (a-f): for binuclear complex **1-6**.

Thermogravimetric Studies for 1-6

All the complexes **1-6** were studied for their thermal behaviour. The thermogravimetric study for **1-6** was performed at a heating rate of 10 °C /min under N_2 atmosphere from room temperature to 550 °C. The TGA/DTA plots and thermal analysis data are given in supplementary information (Fig. S29, Table S2).

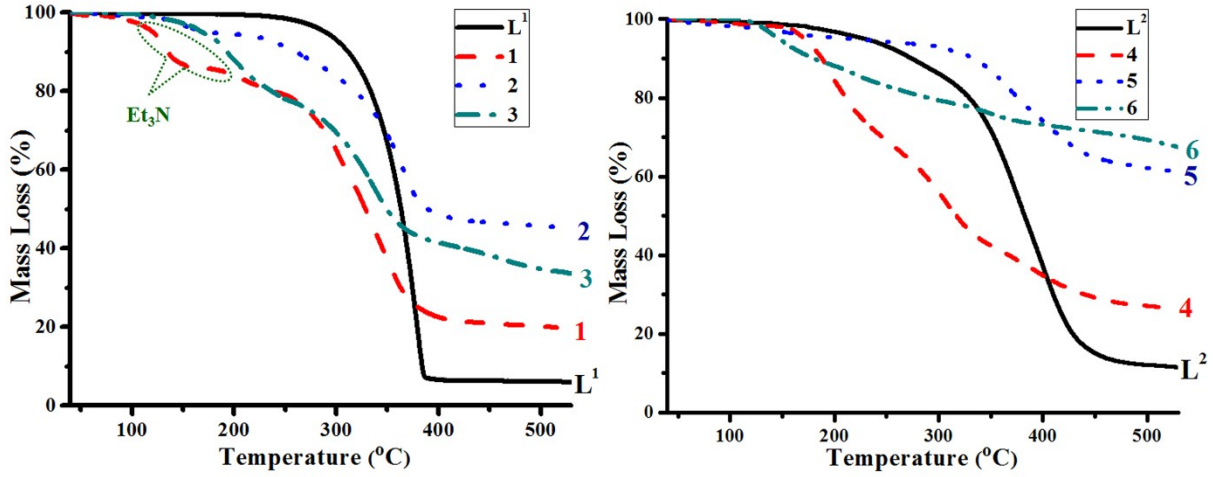

Fig. S30 TG plots (a) **L**[1], **1-3** and (b) **L**[2], **4-6**.

Notably, all the dithiocarbamate complexes **1-6** showed a multistage thermal degradation pattern due to the elimination of different molecular fragments, evidence by TG curves (Fig. S30) which are indeed accompanied by corresponding peaks on DTG curves. This is consistent with the degradation patterns showed by several transition metal dithiocarbamate complexes.[3] Although, the thermal degradation of Zn^{II}/Cd^{II} complexes is continued at 550 °C, however, Ni^{II} complexes **1** and **4** gave a stable residual mass of 20.1% and 29.5 % which correspond to NiS (calc. 14.18 % for **1** and 12.26 % for **4**) plus char, respectively. Reportedly the size and shape of the metal sulfide nanoparticles greatly depend on the nature of organic moiety present in metal dithiocarbamate complexes[4] which consecutively affect the fundamental properties such as optical, electrical and mechanical. The thermogravimetric analysis indicates the suitability complexes **1** and **4** as single source precursors for the synthesis of metal sulphide nano particles and thin films[5] which adds further merit to this work. Moreover, the binuclear Ni^{II}dithiocarbamate macrocycles **1** display first weight loss of 8.4% in the temperature of 100-150°C which can be assigned to the loss of one triethyl amine molecule (calcd. 7.8%). The loss of triethyl amine fragment at much higher temperature than its boiling point confirms the association of **1** and Et_3N. Earlier, the microanalysis and NMR data clearly evident the association of Et_3N molecules with both of the Ni^{II}dithiocarbamate macrocycles **1** and **4**, however the TG curve of 4 could not display the loss of Et_3N molecule distinctly due to continuous mass loss.

Table S3 Thermogravimetric data for **1-6**.

Compounds	Mass Loss% (Temperature °C)	DTG (°C)	Residual content (%)	Inference
1	8.4% (100-150) 79.9% (100-700)	117.8 (26.8), 183.7 (29.5), 213.4 (52.5), 279.2 (81.3), 318.6 (120.9)	20.1	1st stage: loss of Et_3N molecules (calc. 7.8 %). 2nd -4th stage: continuous mass loss of ligand framework. - at 400 °C stable residual mass obtained which corresponds to NiS (14.18 %) and char (5.92 %). - Maximum rate of decomposition observed at 318.6 °C on DTG curve.
2	4.4% (100-200) 47.4% (200-450) 54.2% (100-500)	136.9 (51.2), 353.1 (278.6)	45.8	1st stage: insignificant mass loss of solvent impurities. 2nd stage: continues mass loss of ligand framework even at 550 °C. - Maximum rate of decomposition observed at 353.1 °C on DTG curve.
3	67.1% (120-550)	178.6 (51.4),	32.9	1st -2nd stage: continues mass loss of ligand framework

		316.4 (84.9)		even at 550 °C. - Maximum rate of decomposition observed at 316.4 °C on DTG curve.
4	70.5% (120-500)	192.8(124.6), 304.2(84.8), 319.4(36.2)	29.5	Thermally stable up to 150 °C. 1st -3rd stage: Continuous thermal decomposition which continues after 550 °C. - at 550 °C residual mass obtained which corresponds to NiS (12.26 %) and char (17.24 %). - Maximum rate of decomposition observed at 192.8 °C on DTG curve.
5	2.78% (100-200) 31.57% (280-500) 38.53% (100-500)	304.7(312.3), 362.5(97.1), 410.4(79.4)	61.47	1st -3rd stage: continues mass loss of ligand framework even at 550 °C. - Maximum rate of decomposition observed at 304.7 °C on DTG curve.
6	34.8% (120-550)	130.9(40.8), 209.3(26.0), 344.8(19.6)	65.2	1st -3rd stage: continues mass loss of ligand framework even at 550 °C. - Maximum rate of decomposition observed at 130.9 °C on DTG curve.

IV. Host-Guest Interactions

The host-guest binding ability of some of the macrocyclic complexes (**1-4**) was explored towards a number of guest species viz. 1,4-dioxane, 4,4'-bipyridine, piperazine and triethyl amine by Job plot experiments using UV-vis absorption spectrophotometry.

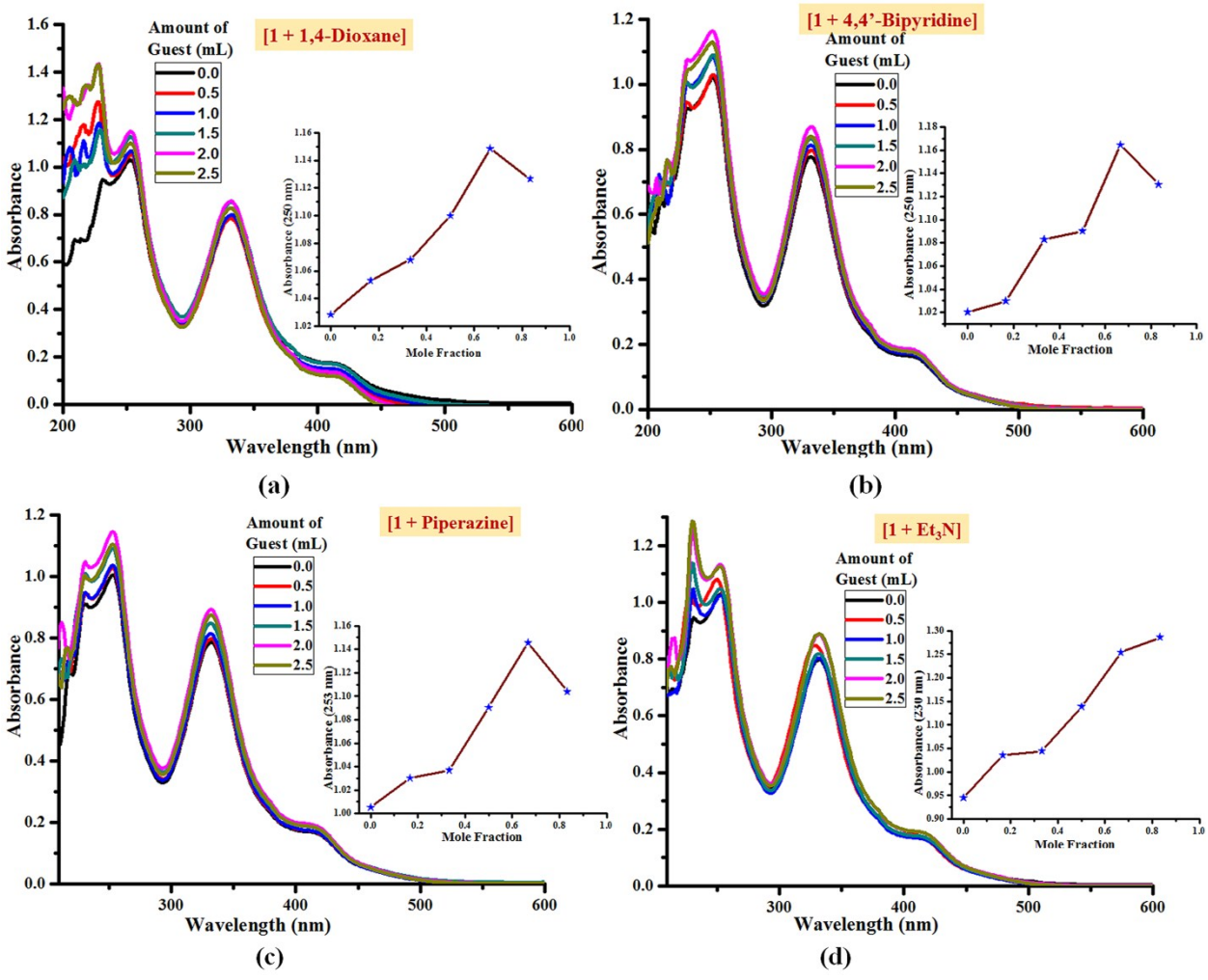

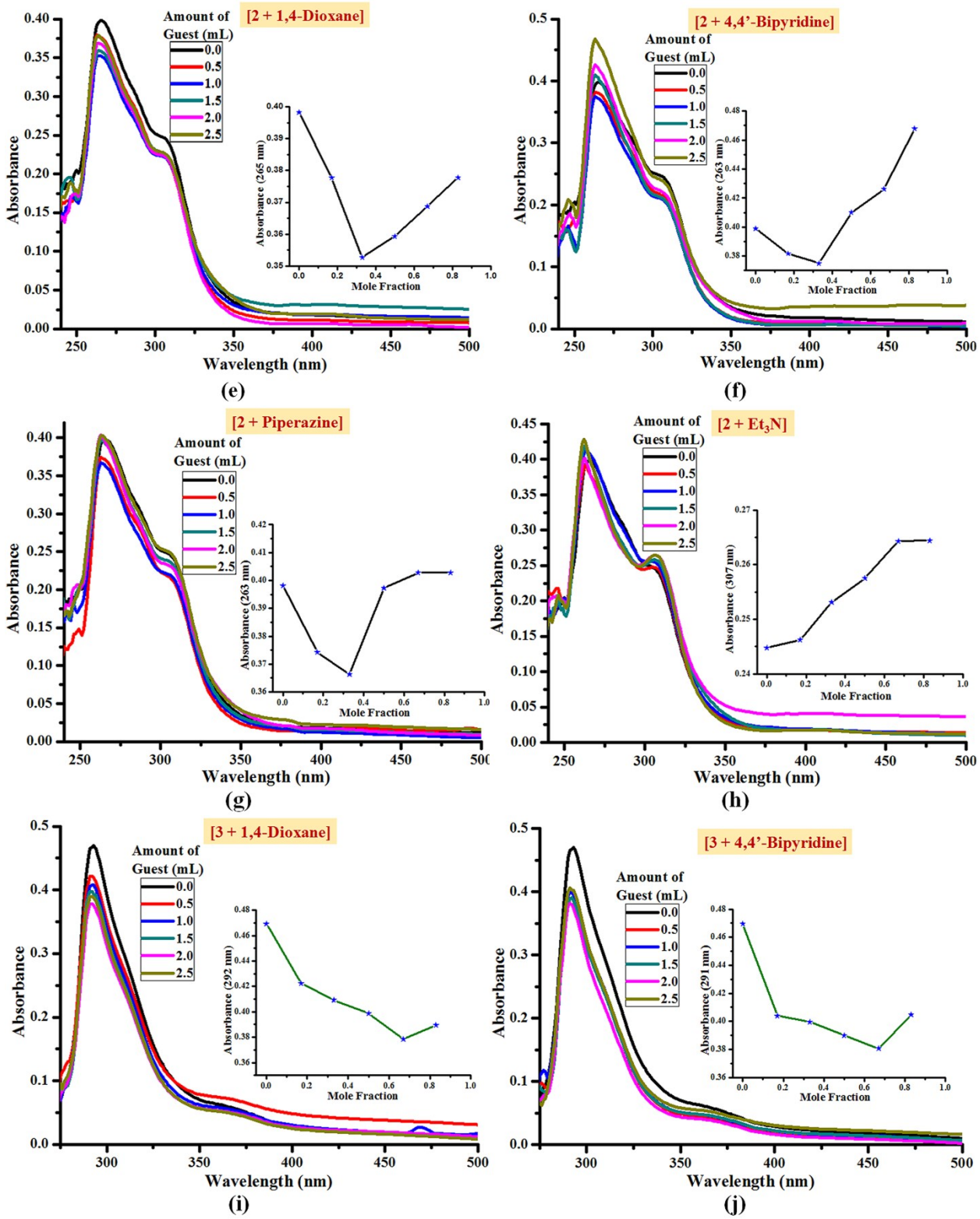
[2 + 1,4-Dioxane]
Amount of Guest (mL)
0.0
0.5
1.0
1.5
2.0
2.5
Absorbance
Wavelength (nm)
Absorbance (265 nm)
Mole Fraction
(e)
[2 + 4,4'-Bipyridine]
Absorbance (263 nm)
(f)
[2 + Piperazine]
Absorbance (263 nm)
(g)
[2 + Et3N]
Absorbance (307 nm)
(h)
[3 + 1,4-Dioxane]
Absorbance (292 nm)
(i)
[3 + 4,4'-Bipyridine]
Absorbance (291 nm)
(j)

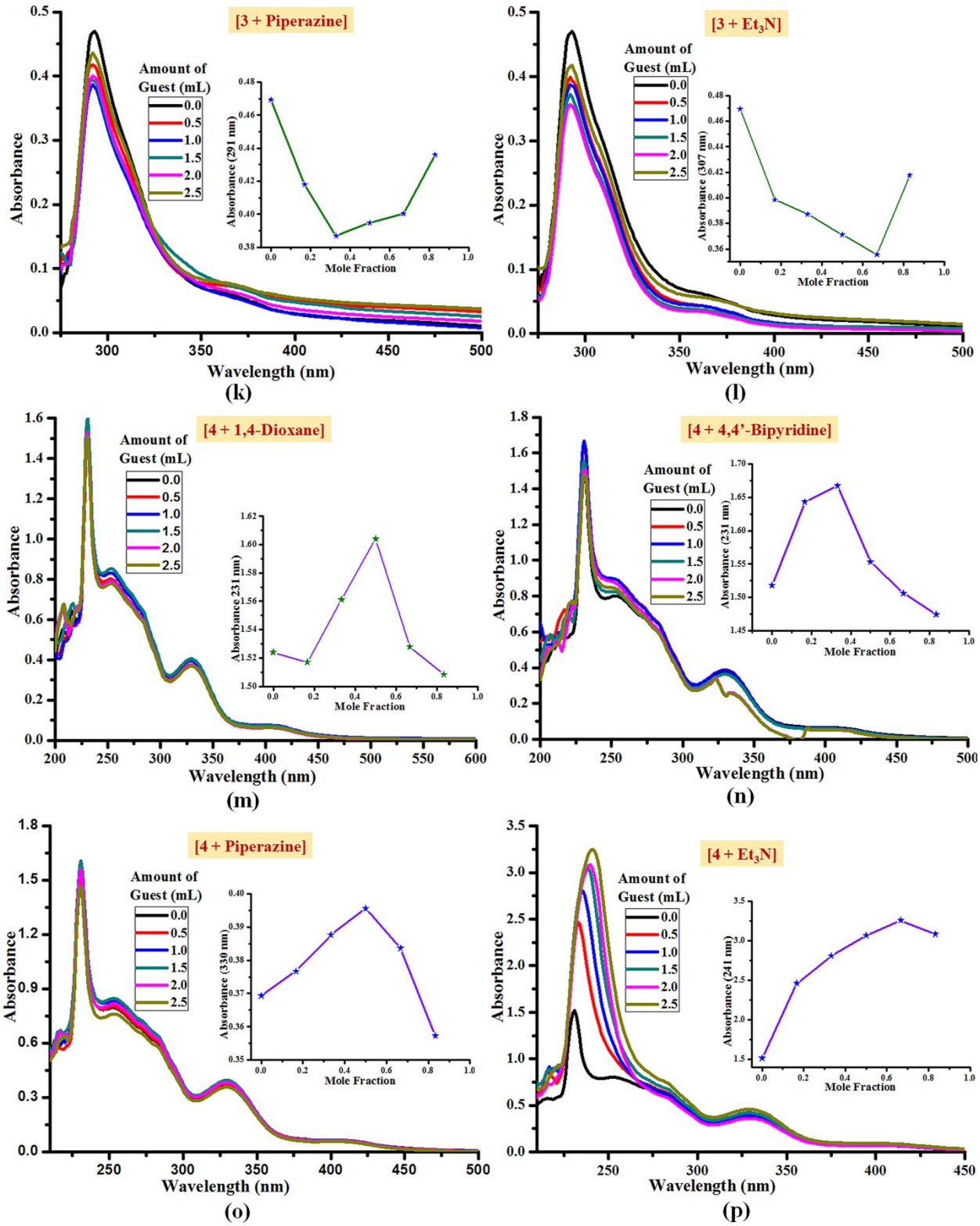

Fig. S31 UV-visible absorption spectral change in Job Plot experiments of **1-4** with various guests. Inset shows the Job Plot for the interaction between hosts and guests consistent with 1:1 (m, o); 1:2 (a-c, i, j. l, p) and 2:1 (e-g, k, n) (host : guest) binding stoichiometries.

V. Computational Investigation

The DFT calculations have been widely used in recent years due to its ability to provide reasonably good results even for huge molecular structures. All the calculations were performed with the Gaussian 03 program suite[28] and molecular orbitals were generated using

GaussView 3.0 program. In search of structural details, we performed a DFT study for geometry optimizations of L^1-$L^2$and 1-6 using B3LYP/6-31G (d, p) and B3LYP/LanL2DZ basis sets, respectively.

1. Cartesian Coordinates for Optimized Geometries

Table S4 Coordinates for optimized geometry of diamine precursor $\mathbf{L^1}$.

Atom Type	Coordinates (Angstroms) X	Y	Z
C1	-3.8022	0.8754	-0.1235
C2	-2.7524	0.1733	0.4917
C3	-1.4692	0.7191	0.5653
C4	-1.2099	1.9776	0.0247
C5	-2.2453	2.6921	-0.5841
C6	-3.5217	2.1495	-0.6541
H7	-2.9269	-0.8038	0.9277
H8	-0.6742	0.1648	1.0523
H9	-2.0346	3.6746	-0.9938
H10	-4.3173	2.7118	-1.1369
O11	0.0163	2.6132	0.1247
C12	1.1834	1.8703	0.0508
C13	2.1986	2.1658	0.9554
C14	1.4045	0.915	-0.9478
C15	3.4336	1.5201	0.8714
H16	2.0197	2.9179	1.7168
C17	2.6261	0.2583	-1.0191
H18	0.6198	0.689	-1.6621
C19	3.666	0.5439	-0.1119
H20	4.2098	1.7819	1.5812
H21	2.7864	-0.4902	-1.7915
N22	-5.0904	0.345	-0.2614
H23	-5.8086	1.0534	-0.3427
N24	4.8631	-0.1738	-0.1981
H25	5.057	-0.5261	-1.1268
C26	6.0618	0.2756	0.497
H27	6.3339	1.3134	0.2399
H28	5.8521	0.27	1.5755
C29	-5.5184	-0.7976	0.5348
H30	-4.8819	-1.6538	0.2724
H31	-5.3828	-0.6318	1.6172
C32	7.2315	-0.6429	0.2109
C33	8.4635	-0.1242	-0.2011
C34	7.1015	-2.0302	0.3691
C35	9.5485	-0.9692	-0.4434
C36	8.1818	-2.8761	0.1225
H37	6.1452	-2.4394	0.6816
C38	9.4098	-2.3477	-0.283
H39	8.0669	-3.9488	0.2494
H40	10.2514	-3.0071	-0.4741
C41	-6.9647	-1.1465	0.2514
C42	-7.8731	-1.3318	1.299
C43	-7.4135	-1.3054	-1.0676
C44	-9.2011	-1.6769	1.0396
C45	-8.7402	-1.6444	-1.329
H46	-6.7146	-1.1554	-1.8853
C47	-9.6382	-1.8331	-0.2756
H48	-9.0739	-1.7645	-2.3558
H49	-10.6714	-2.0981	-0.4799
H50	-9.8932	-1.817	1.8649
H51	-7.5386	-1.2041	2.3254
H52	8.5741	0.9491	-0.3342

H53	10.4982	-0.5499	-0.7628

Table S5 Coordinates for optimized geometry of diamine precursor $\mathbf{L^2}$.

Atom Type	Coordinates (Angstroms) X	Y	Z
C1	-3.8712	-1.5536	0.1586
C2	-2.9251	-0.6282	-0.3127
C3	-1.6045	-1.0115	-0.554
C4	-1.2033	-2.3275	-0.3294
C5	-2.1343	-3.2626	0.1302
C6	-3.4482	-2.8804	0.3674
H7	-3.2098	0.3998	-0.5051
H8	-0.89	-0.2844	-0.9249
H9	-1.8137	-4.2863	0.2932
H10	-4.1618	-3.6146	0.7336
O11	0.0687	-2.7925	-0.6181
C12	1.1696	-1.9987	-0.3415
C13	2.2079	-1.9915	-1.2682
C14	1.3102	-1.2917	0.8581
C15	3.386	-1.2892	-1.0084
H16	2.0925	-2.5541	-2.1888
C17	2.4748	-0.577	1.1066
H18	0.5093	-1.3021	1.5896
C19	3.5367	-0.5579	0.1812
H20	4.1813	-1.3152	-1.7442
H21	2.5718	-0.0215	2.0365
N22	-5.1939	-1.2061	0.4666
H23	-5.8304	-1.9895	0.3854
N24	4.6707	0.2149	0.4669
H25	4.8249	0.324	1.4619
C26	5.9117	0.0042	-0.2609
H27	6.2595	-1.037	-0.1658
H28	5.716	0.1624	-1.3303
C29	-5.7743	0.027	-0.0399
H30	-5.1588	0.8672	0.3096
H31	-5.7416	0.0631	-1.1407
C32	7.0071	0.9596	0.18
C33	8.3829	0.6554	-0.0958
C34	6.6934	2.1443	0.8167
C35	8.7996	-0.5183	-0.7849
C36	9.397	1.5796	0.328
C37	7.6965	3.0521	1.231
H38	5.651	2.3882	0.9918
C39	10.1315	-0.7707	-1.0306
H40	8.0594	-1.23	-1.1332
C41	10.7613	1.2854	0.0634
C42	9.0205	2.7742	0.9982
H43	7.4081	3.9708	1.7332
C44	11.1259	0.1371	-0.6004
H45	10.4202	-1.6742	-1.5597
H46	11.5168	1.9932	0.3947
H47	9.7978	3.4643	1.3151
H48	12.1728	-0.0735	-0.7973
C49	-7.1992	0.232	0.4456
C50	-8.0796	1.1257	-0.2527
C51	-7.6527	-0.4102	1.5811
C52	-7.6888	1.8647	-1.4047
C53	-9.4195	1.3011	0.2336
C54	-8.9731	-0.2321	2.0571
H55	-6.9739	-1.0583	2.1249
C56	-8.5662	2.7129	-2.0441

H57	-6.6795	1.769	-1.7888
C58	-10.2998	2.1792	-0.4532
C59	-9.841	0.6002	1.3951
H60	-9.2919	-0.7593	2.9515
C61	-9.8876	2.8716	-1.568
H62	-8.24	3.2647	-2.9208
H63	-11.3119	2.2973	-0.0748
H64	-10.8579	0.7414	1.7516
H65	-10.5713	3.541	-2.0815

Table S6 Coordinates for optimized geometry of binuclear Ni^{II}dithiocarbamate complex **1**.

Atom Type	Coordinates (Angstroms) X	Y	Z
C1	-0.5697	6.49	-1.6208
C2	-0.9645	5.7982	-0.4714
C3	-0.0089	5.1371	0.3045
C4	1.3289	5.134	-0.0823
C5	1.7161	5.821	-1.2363
C6	0.7707	6.5105	-1.9995
O7	3.0335	5.8955	-1.6563
C8	3.8123	4.749	-1.5651
C9	4.6449	4.55	-0.4644
C10	5.4216	3.3922	-0.3889
C11	5.3815	2.4588	-1.4284
C12	4.5813	2.69	-2.553
C13	3.786	3.8304	-2.6165
N14	-2.3547	5.7899	-0.0874
N15	6.1729	1.2543	-1.3515
C16	-2.9327	7.0864	0.3471
C17	-2.4285	7.5299	1.7059
C18	7.6347	1.3881	-1.557
C19	8.392	1.9378	-0.3634
C20	-3.066	4.6469	-0.0734
C21	5.5764	0.0583	-1.1731
S22	-2.4076	3.1123	-0.5134
S23	-4.7342	4.5413	0.3864
S24	3.8656	-0.1318	-1.051
S25	6.4283	-1.4433	-1.0416
C26	-2.8906	6.9062	2.8744
C27	-2.4215	7.3134	4.1229
C28	-1.4884	8.3496	4.2203
C29	-1.0253	8.9759	3.0627
C30	-1.4929	8.5651	1.8124
C31	9.126	3.1234	-0.4814
C32	9.8485	3.6253	0.6038
C33	9.8362	2.9472	1.8229
C34	9.1037	1.763	1.9501
C35	8.3894	1.258	0.8642
C36	0.149	-5.1277	0.7003
C37	0.8708	-5.8559	-0.2489
C38	0.1916	-6.6311	-1.194
C39	-1.2009	-6.6693	-1.1983
C40	-1.9163	-5.9141	-0.2661
C41	-1.2435	-5.1427	0.6855
O42	-3.2974	-6.0082	-0.3108
C43	-4.0348	-4.8482	-0.1124
C44	-4.5537	-4.5534	1.1486
C45	-5.2939	-3.3841	1.3273
C46	-5.5344	-2.5352	0.2437
C47	-5.0564	-2.8654	-1.0282
C48	-4.2941	-4.0169	-1.2036

N49	2.3129	-5.8304	-0.2534
N50	-6.2835	-1.3206	0.448
C51	3.0013	-7.0987	0.0937
C52	2.8849	-7.447	1.5642
C53	-7.7313	-1.4649	0.7341
C54	-8.5345	-1.8777	-0.4834
C55	2.9893	-4.6949	-0.5107
C56	-5.6806	-0.1191	0.3486
S57	2.2215	-3.1869	-0.8557
S58	4.7185	-4.574	-0.534
S59	-4.0085	0.0669	-0.0374
S60	-6.4804	1.396	0.6002
C61	2.0366	-8.4774	1.9847
C62	1.9263	-8.8004	3.339
C63	2.6631	-8.0901	4.2873
C64	3.5113	-7.058	3.8762
C65	3.6237	-6.7386	2.5234
C66	-9.0669	-3.1682	-0.5783
C67	-9.8094	-3.5512	-1.6977
C68	-10.0218	-2.6446	-2.7366
C69	-9.4916	-1.3539	-2.6508
C70	-8.7542	-0.9709	-1.531
H71	-1.3126	6.9915	-2.2341
H72	-0.3152	4.6143	1.2034
H73	2.0632	4.6009	0.5108
H74	1.0942	7.0344	-2.8929
H75	4.6686	5.2888	0.3303
H76	6.0435	3.2077	0.4794
H77	4.5636	1.9632	-3.3583
H78	3.1416	4.0149	-3.4698
H79	-4.0184	6.973	0.3457
H80	-2.6734	7.8297	-0.4126
H81	8.0073	0.3964	-1.8272
H82	7.7739	2.0434	-2.4229
H83	-3.6202	6.1039	2.8008
H84	-2.789	6.825	5.0214
H85	-1.1268	8.6677	5.1945
H86	-0.3006	9.7828	3.1301
H87	-1.1274	9.0529	0.9117
H88	9.1324	3.6587	-1.4283
H89	10.4147	4.5465	0.4961
H90	10.3947	3.3365	2.6698
H91	9.0942	1.2276	2.8957
H92	7.8297	0.3317	0.9635
H93	0.6771	-4.5388	1.4416
H94	0.7494	-7.1852	-1.9434
H95	-1.7446	-7.2581	-1.9298
H96	-1.7995	-4.5583	1.4097
H97	-4.3614	-5.2256	1.9787
H98	-5.6659	-3.1212	2.3132
H99	-5.2652	-2.2105	-1.8666
H100	-3.8969	-4.2791	-2.1787
H101	2.5572	-7.8897	-0.5177
H102	4.0457	-6.9929	-0.2059
H103	-7.8352	-2.2129	1.526
H104	-8.0779	-0.5085	1.131
H105	1.4579	-9.0304	1.2484
H106	1.2652	-9.6046	3.6505
H107	2.5797	-8.3398	5.3417
H108	4.0908	-6.5042	4.6099
H109	4.2882	-5.9396	2.2047
H110	-8.9002	-3.8785	0.2284

H111	-10.2185	-4.5562	-1.7568
H112	-10.5991	-2.9398	-3.6087
H113	-9.658	-0.6422	-3.455
H114	-8.3489	0.0355	-1.4629
Ni115	-4.4301	2.2922	0.0982
Ni116	4.3266	-2.348	-0.8863

Table S7 Coordinates for optimized geometry of binuclear Zn^{II}dithiocarbamate complex **2**.

Atom	Coordinates (Angstroms)		
Type	X	Y	Z
C1	5.7077	-3.4506	-0.637
C2	5.1249	-2.5148	-1.4928
C3	3.8739	-2.7662	-2.0664
C4	3.1833	-3.9307	-1.7527
C5	3.7536	-4.8477	-0.8629
C6	5.0182	-4.6227	-0.3197
O7	3.0994	-6.0228	-0.5338
C8	1.7783	-5.9326	-0.1334
C9	1.3451	-4.9287	0.7396
C10	0.0113	-4.8902	1.1292
C11	-0.8895	-5.8437	0.646
C12	-0.4454	-6.864	-0.197
C13	0.8928	-6.9103	-0.5899
N14	5.8023	-1.282	-1.8244
N15	-2.2737	-5.7804	1.0545
C16	6.7874	-1.3637	-2.931
C17	8.114	-1.9685	-2.514
C18	-2.6652	-6.71	2.1454
C19	-2.0457	-6.3649	3.4851
C20	5.4606	-0.1291	-1.2126
C21	-3.1089	-4.8686	0.5159
S22	6.1306	1.4017	-1.7289
S23	4.3239	-0.1583	0.1018
S24	-2.5747	-3.8968	-0.8234
S25	-4.7237	-4.6371	1.1469
C26	8.5371	-3.1887	-3.0528
C27	9.7664	-3.7417	-2.6858
C28	10.5822	-3.08	-1.7678
C29	10.1662	-1.8615	-1.2226
C30	8.9424	-1.3068	-1.5949
C31	-1.0272	-7.1617	4.0202
C32	-0.4567	-6.8535	5.2572
C33	-0.898	-5.7382	5.9697
C34	-1.9134	-4.9353	5.4422
C35	-2.4864	-5.2469	4.2095
C36	-4.0658	2.4433	-1.8584
C37	-5.3272	2.1555	-1.3263
C38	-5.921	3.0272	-0.4124
C39	-5.2323	4.1685	0.0036
C40	-3.9576	4.4275	-0.4998
C41	-3.3758	3.5771	-1.4466
O42	-3.3054	5.5709	-0.0712
C43	-1.9868	5.4469	0.3292
C44	-1.5648	4.3804	1.1313
C45	-0.2335	4.3088	1.5236
C46	0.675	5.2913	1.1167
C47	0.2431	6.371	0.3447
C48	-1.0933	6.4487	-0.0515
N49	-6.0031	0.9553	-1.7638
N50	2.0515	5.179	1.5437
C51	-6.9692	1.1279	-2.8765

C52	-8.3001	1.7045	-2.4339
C53	2.4065	5.9368	2.7689
C54	2.6054	7.4198	2.5248
C55	-5.6723	-0.2442	-1.242
C56	2.898	4.3347	0.9189
S57	-6.3273	-1.7271	-1.8978
S58	-4.5635	-0.3236	0.0942
S59	2.3863	3.518	-0.5282
S60	4.5013	4.0323	1.5484
C61	-8.717	2.9589	-2.8927
C62	-9.9502	3.4867	-2.5018
C63	-10.7758	2.7647	-1.6399
C64	-10.366	1.5114	-1.1746
C65	-9.1384	0.9824	-1.571
C66	3.6621	7.8757	1.7221
C67	3.8479	9.2413	1.5102
C68	2.9858	10.1694	2.1023
C69	1.9357	9.7243	2.9053
C70	1.746	8.3555	3.1111
H71	6.679	-3.2495	-0.1988
H72	3.4348	-2.0338	-2.7367
H73	2.203	-4.1237	-2.1757
H74	5.4412	-5.3548	0.3604
H75	2.0446	-4.1827	1.1008
H76	-0.3402	-4.1132	1.7992
H77	-1.1496	-7.6005	-0.5726
H78	1.255	-7.6816	-1.2617
H79	6.9242	-0.3516	-3.317
H80	6.3306	-1.9694	-3.7199
H81	-3.7546	-6.7017	2.2011
H82	-2.3491	-7.7111	1.8341
H83	7.9015	-3.71	-3.7649
H84	10.0819	-4.6891	-3.1145
H85	11.5381	-3.5085	-1.4789
H86	10.7999	-1.339	-0.511
H87	8.6269	-0.3542	-1.1774
H88	-0.6771	-8.029	3.4653
H89	0.3323	-7.4828	5.6602
H90	-0.4555	-5.4955	6.9322
H91	-2.2647	-4.0683	5.9953
H92	-3.2824	-4.6276	3.8047
H93	-3.6185	1.7616	-2.5752
H94	-6.9003	2.799	-0.0067
H95	-5.664	4.8496	0.7297
H96	-2.3881	3.7964	-1.8381
H97	-2.2693	3.6115	1.4297
H98	0.1125	3.4771	2.1297
H99	0.952	7.1304	0.034
H100	-1.4481	7.2684	-0.6676
H101	-6.4975	1.7907	-3.6086
H102	-7.1036	0.1494	-3.3423
H103	1.5946	5.7799	3.4862
H104	3.3122	5.4842	3.1777
H105	-8.0737	3.5271	-3.5608
H106	-10.2609	4.4615	-2.868
H107	-11.7346	3.1734	-1.3325
H108	-11.0073	0.9421	-0.5071
H109	-8.8278	0.0032	-1.2159
H110	4.3402	7.1572	1.2688
H111	4.6707	9.5825	0.8877
H112	3.1349	11.2334	1.9387
H113	1.2609	10.4388	3.369

H114	0.9226	8.0117	3.733
Zn115	4.4544	2.269	-0.159
Zn116	-4.6699	-2.7202	-0.3842

Table S8 Coordinates for optimized geometry of binuclear Cd^{II}dithiocarbamate complex **3**.

Atom	Coordinates (Angstroms)		
Type	X	Y	Z
C1	0.123	6.7991	-0.0125
C2	-0.3784	5.8289	0.8568
C3	0.4533	4.8051	1.3208
C4	1.77	4.7228	0.8829
C5	2.2568	5.6759	-0.0181
C6	1.4449	6.724	-0.4538
O7	3.5657	5.6408	-0.466
C8	4.0743	4.4182	-0.8697
C9	5.352	4.0635	-0.437
C10	5.9026	2.8436	-0.8345
C11	5.1697	1.988	-1.6584
C12	3.905	2.3678	-2.1201
C13	3.3518	3.5806	-1.7269
N14	-1.7481	5.8912	1.3114
N15	5.7083	0.7149	-2.0814
C16	-2.0112	6.8528	2.4134
C17	-1.3987	6.4394	3.7372
C18	6.5847	0.7604	-3.2774
C19	7.9813	1.2717	-2.9824
C20	-2.6849	5.0631	0.7979
C21	5.3296	-0.4302	-1.4705
S22	-2.2616	4.0605	-0.5597
S23	-4.2911	5.0027	1.4848
S24	4.3222	-0.3351	-0.0577
S25	5.8387	-1.9802	-2.1026
C26	-1.9536	5.3895	4.4849
C27	-1.3865	5.0149	5.7027
C28	-0.262	5.6858	6.1918
C29	0.2937	6.7331	5.4562
C30	-0.2722	7.1047	4.2347
C31	8.4323	2.4683	-3.5504
C32	9.7244	2.9352	-3.2969
C33	10.5766	2.2103	-2.4637
C34	10.1332	1.015	-1.8895
C35	8.8461	0.546	-2.1492
C36	-0.7804	-4.7552	1.6275
C37	0.0101	-5.7882	1.1145
C38	-0.5654	-6.7844	0.324
C39	-1.9244	-6.7284	0.0108
C40	-2.6982	-5.6727	0.4943
C41	-2.1337	-4.6917	1.3165
O42	-4.0454	-5.6559	0.1771
C43	-4.5936	-4.4531	-0.2331
C44	-5.8323	-4.0845	0.2932
C45	-6.4205	-2.8842	-0.1085
C46	-5.769	-2.0621	-1.0294
C47	-4.5475	-2.4583	-1.5827
C48	-3.9548	-3.6507	-1.1845
N49	1.4169	-5.8354	1.4395
N50	-6.3631	-0.8121	-1.4441
C51	1.7872	-6.7711	2.5327
C52	1.2952	-6.3318	3.8978
C53	-7.4391	-0.924	-2.4616
C54	-6.9425	-1.3771	-3.8205

C55	2.2984	-5.0199	0.8188
C56	-5.8982	0.3642	-0.9666
S57	1.7439	-4.0478	-0.5132
S58	3.9641	-4.9459	1.3443
S59	-4.7129	0.3458	0.3044
S60	-6.4793	1.8781	-1.6235
C61	0.2337	-7.0016	4.5169
C62	-0.2204	-6.6066	5.7773
C63	0.3828	-5.5311	6.43
C64	1.4428	-4.8553	5.8188
C65	1.8987	-5.2535	4.5624
C66	-7.2471	-2.6584	-4.2936
C67	-6.8005	-3.0802	-5.5479
C68	-6.0377	-2.2226	-6.3408
C69	-5.7275	-0.9412	-5.8763
C70	-6.1786	-0.5189	-4.626
H71	-0.5273	7.5913	-0.3718
H72	0.0594	4.0678	2.0119
H73	2.4155	3.9218	1.2273
H74	1.8482	7.4545	-1.1474
H75	5.8949	4.7356	0.2195
H76	6.8841	2.5451	-0.4831
H77	3.3474	1.6977	-2.7674
H78	2.3631	3.8722	-2.0651
H79	-3.0934	6.9611	2.4967
H80	-1.5967	7.8149	2.0955
H81	6.6188	-0.2493	-3.6914
H82	6.094	1.4113	-4.0082
H83	-2.8332	4.8735	4.1097
H84	-1.8268	4.2022	6.2743
H85	0.1762	5.3943	7.1426
H86	1.1673	7.2605	5.8298
H87	0.1656	7.9195	3.6625
H88	7.7685	3.0393	-4.1956
H89	10.0604	3.8656	-3.7468
H90	11.5814	2.5719	-2.2626
H91	10.7944	0.4435	-1.2435
H92	8.508	-0.389	-1.7097
H93	-0.3277	-3.9971	2.2573
H94	0.0531	-7.5833	-0.0744
H95	-2.3873	-7.4801	-0.6201
H96	-2.749	-3.8839	1.6984
H97	-6.3105	-4.7276	1.0247
H98	-7.3678	-2.5712	0.3207
H99	-4.0598	-1.8219	-2.313
H100	-2.9996	-3.9559	-1.5984
H101	1.353	-7.7426	2.2754
H102	2.8733	-6.8708	2.5188
H103	-8.1671	-1.6434	-2.0724
H104	-7.9266	0.0498	-2.5248
H105	-0.2415	-7.8381	4.0095
H106	-1.0446	-7.1379	6.2455
H107	0.0317	-5.2215	7.4107
H108	1.9202	-4.0204	6.3249
H109	2.7292	-4.7333	4.0927
H110	-7.838	-3.3316	-3.6766
H111	-7.0468	-4.0777	-5.9019
H112	-5.688	-2.5483	-7.3168
H113	-5.1388	-0.2666	-6.4923
H114	-5.946	0.4814	-4.2707
Cd115	-4.5857	2.933	-0.1273
Cd116	4.1105	-2.9357	-0.3598

Table S9 Coordinates for optimized geometry of binuclear Ni^{II}dithiocarbamate complex **4**.

Atom Type	Coordinates (Angstroms) X	Y	Z
C1	-2.7944	4.8117	2.4243
C2	-3.1553	3.6896	1.6657
C3	-2.6885	2.4277	2.0594
C4	-1.8491	2.2952	3.1578
C5	-1.4075	3.433	3.8418
C6	-1.9104	4.6876	3.4977
O7	-0.4965	3.3683	4.8821
C8	0.5062	2.4195	4.8358
C9	0.9488	1.8919	6.0508
C10	1.9124	0.8811	6.055
C11	2.4164	0.3863	4.8495
C12	2.0252	0.9748	3.6428
C13	1.0951	2.0057	3.6346
N14	-3.8413	3.862	0.4097
N15	3.2192	-0.8129	4.8264
C16	-3.3904	4.9925	-0.4288
C17	-4.2987	6.2118	-0.3903
C18	2.4833	-2.0788	5.1318
C19	1.5019	-2.499	4.0446
C20	-4.673	2.9358	-0.1301
C21	4.4614	-0.8248	4.3052
S22	-4.9156	2.7766	-1.8405
S23	-5.5354	1.7314	0.7629
S24	5.3173	0.6035	3.8305
S25	5.3393	-2.2767	3.9251
C26	-3.9134	7.3763	-1.1347
C27	-4.7641	8.5316	-1.1039
C28	-5.965	8.4947	-0.3443
C29	-6.3114	7.3656	0.3563
C30	-5.4736	6.2238	0.3323
C31	1.9927	-3.2086	2.9612
C32	1.1561	-3.6189	1.8986
C33	-0.1848	-3.3172	1.9219
C34	-0.7466	-2.6102	3.0173
C35	0.098	-2.1958	4.1066
C36	3.5896	-1.8835	-1.3506
C37	4.6736	-1.4634	-2.133
C38	4.671	-1.7417	-3.5053
C39	3.5756	-2.3742	-4.0956
C40	2.4848	-2.7554	-3.3126
C41	2.5156	-2.5485	-1.9288
O42	1.4263	-3.3674	-3.9575
C43	0.1353	-3.1873	-3.5012
C44	-0.763	-4.238	-3.6987
C45	-2.0799	-4.1238	-3.2513
C46	-2.5025	-2.9692	-2.5807
C47	-1.6026	-1.9075	-2.4182
C48	-0.3029	-2.0019	-2.9
N49	5.6879	-0.6122	-1.5647
N50	-3.7857	-2.9352	-1.9264
C51	5.9728	0.6417	-2.291
C52	7.2552	0.6242	-3.1088
C53	-4.1347	-4.1068	-1.0987
C54	-5.1285	-5.0652	-1.7382
C55	6.1835	-0.787	-0.314
C56	-4.5521	-1.8184	-1.8599

S57	6.804	0.516	0.6458
S58	6.1845	-2.2923	0.5347
S59	-4.46	-0.5008	-2.973
S60	-5.6897	-1.5291	-0.5855
C61	7.5802	1.7781	-3.8971
C62	8.7876	1.7705	-4.6725
C63	9.6326	0.6279	-4.6382
C64	9.2998	-0.4614	-3.8713
C65	8.1071	-0.4607	-3.1071
C66	-5.6897	-4.8174	-2.9736
C67	-6.6181	-5.7165	-3.5537
C68	-6.9787	-6.8639	-2.8911
C69	-6.4276	-7.1634	-1.6155
C70	-5.4884	-6.2552	-1.0221
C71	-2.7213	7.4419	-1.9087
C72	-2.3862	8.5814	-2.6088
C73	-3.2256	9.7185	-2.5728
C74	-4.3881	9.6892	-1.8359
C75	-2.136	-2.3108	3.0537
C76	-2.6938	-1.6436	4.1196
C77	-1.8729	-1.2489	5.2025
C78	-0.5208	-1.5155	5.1936
C79	6.7588	2.9388	-3.9471
C80	7.106	4.027	-4.7192
C81	8.2948	4.0136	-5.4844
C82	9.1145	2.9078	-5.4578
C83	-6.7883	-8.3442	-0.9134
C84	-6.2536	-8.628	0.3232
C85	-5.3296	-7.7349	0.9126
C86	-4.9577	-6.5803	0.2573
H87	-3.1712	5.7931	2.1557
H88	-2.9643	1.5428	1.5017
H89	-1.501	1.31	3.4459
H90	-1.5906	5.5612	4.0563
H91	0.5145	2.2558	6.9762
H92	2.2429	0.4522	6.9968
H93	2.4405	0.6126	2.7095
H94	0.7894	2.4492	2.6946
H95	-2.3841	5.2545	-0.0906
H96	-3.2945	4.6247	-1.4559
H97	3.235	-2.8556	5.2737
H98	1.9863	-1.93	6.0917
H99	-6.6033	9.3747	-0.33
H100	-7.2309	7.3364	0.934
H101	-5.7706	5.343	0.8926
H102	3.0495	-3.4514	2.9257
H103	1.5832	-4.1808	1.0723
H104	-0.8377	-3.6224	1.1073
H105	3.5753	-1.6818	-0.2869
H106	5.5105	-1.4363	-4.1217
H107	3.5524	-2.5626	-5.1639
H108	1.685	-2.8602	-1.3061
H109	-0.4197	-5.1426	-4.1898
H110	-2.7704	-4.948	-3.3994
H111	-1.9129	-1.0055	-1.9058
H112	0.3781	-1.1694	-2.7683
H113	5.1115	0.8324	-2.9376
H114	6.0053	1.4522	-1.5545
H115	-3.1967	-4.6241	-0.8768
H116	-4.53	-3.7358	-0.1463
H117	10.5464	0.634	-5.2273
H118	9.9478	-1.3327	-3.8418

H119	7.8679	-1.3326	-2.5067
H120	-5.4244	-3.9151	-3.5152
H121	-7.0422	-5.4858	-4.5267
H122	-7.6912	-7.558	-3.3299
H123	-2.0605	6.5822	-1.9588
H124	-1.4712	8.6057	-3.1943
H125	-2.9514	10.611	-3.1284
H126	-5.0418	10.5577	-1.8038
H127	-2.757	-2.6228	2.2171
H128	-3.7571	-1.4227	4.1337
H129	-2.3129	-0.729	6.0492
H130	0.0784	-1.1848	6.0328
H131	5.8428	2.9792	-3.366
H132	6.4627	4.9025	-4.7388
H133	8.5586	4.8768	-6.0892
H134	10.0325	2.8888	-6.0406
H135	-7.5013	-9.0238	-1.3741
H136	-6.5399	-9.5348	0.8487
H137	-4.9111	-7.9598	1.8898
H138	-4.2497	-5.9109	0.7354
Ni139	6.1824	-0.8858	2.3313
Ni140	-5.3904	0.6376	-1.2329

Table S10 Coordinates for optimized geometry of binuclear Zn^{II}dithiocarbamate complex **5**.

Atom	**Coordinates (Angstroms)**		
Type	**X**	**Y**	**Z**
C1	5.6528	-3.4312	-0.8231
C2	4.9621	-2.3965	-1.4569
C3	3.6387	-2.5888	-1.8686
C4	2.9916	-3.7918	-1.614
C5	3.6774	-4.8134	-0.9467
C6	5.0088	-4.643	-0.5667
O7	3.0884	-6.038	-0.6914
C8	1.7673	-6.0529	-0.2801
C9	0.9016	-6.9598	-0.8927
C10	-0.4348	-7.0101	-0.4942
C11	-0.8947	-6.1555	0.5095
C12	-0.0133	-5.2753	1.1439
C13	1.3194	-5.2214	0.7516
N14	5.6062	-1.1356	-1.7536
N15	-2.2819	-6.1807	0.911
C16	6.5802	-1.1468	-2.8609
C17	8.0379	-1.268	-2.4387
C18	-2.6615	-7.2215	1.904
C19	-2.1078	-6.9764	3.2979
C20	5.2127	0.0076	-1.1455
C21	-3.1423	-5.2595	0.4309
S22	5.7705	1.5547	-1.7235
S23	4.142	-0.0625	0.222
S24	-4.7888	-5.1603	1.0129
S25	-2.608	-4.1413	-0.789
C26	9.0285	-1.5025	-3.4495
C27	10.4053	-1.615	-3.0592
C28	10.7559	-1.4838	-1.6883
C29	9.7888	-1.2466	-0.7427
C30	8.4289	-1.1378	-1.1225
C31	-2.7679	-6.0694	4.1094
C32	-2.3279	-5.7936	5.423
C33	-1.2273	-6.4436	5.93
C34	-0.5185	-7.3888	5.1434

C35	-0.951	-7.6628	3.799
C36	-6.3137	2.4596	-0.2788
C37	-5.6761	1.696	-1.2575
C38	-4.4471	2.1077	-1.783
C39	-3.8336	3.2606	-1.3059
C40	-4.4564	3.9997	-0.2942
C41	-5.7004	3.6149	0.2073
O42	-3.8865	5.1572	0.2053
C43	-2.5409	5.1372	0.5232
C44	-1.9578	4.0491	1.183
C45	-0.6051	4.0873	1.4982
C46	0.1698	5.2012	1.1554
C47	-0.425	6.2996	0.5321
C48	-1.7841	6.2676	0.2142
N49	-6.2686	0.478	-1.7604
N50	1.5719	5.2092	1.5109
C51	-7.1509	0.6194	-2.9486
C52	-8.5351	1.1537	-2.6217
C53	1.9483	6.0547	2.6593
C54	2.4991	7.4273	2.2974
C55	-5.9132	-0.7134	-1.2368
C56	2.4472	4.3682	0.9125
S57	-4.8828	-0.7618	0.1636
S58	-6.4458	-2.2173	-1.9534
S59	1.9682	3.4828	-0.5046
S60	4.056	4.1647	1.5513
C61	-8.9099	2.5193	-2.8539
C62	-10.2566	2.9231	-2.5491
C63	-11.1685	1.9767	-2.0129
C64	-10.7801	0.6767	-1.7885
C65	-9.4646	0.2693	-2.1021
C66	2.841	7.7575	1.0026
C67	3.3549	9.0368	0.6785
C68	3.5263	9.9835	1.6584
C69	3.1994	9.6883	3.0095
C70	2.6827	8.3913	3.3437
C71	8.7133	-1.6252	-4.8319
C72	9.6956	-1.8519	-5.7722
C73	11.0495	-1.969	-5.3818
C74	11.3916	-1.8518	-4.0536
C75	0.6159	-8.0682	5.6655
C76	1.3093	-8.9816	4.9066
C77	0.8942	-9.2503	3.5811
C78	-0.2008	-8.61	3.0446
C79	-8.025	3.5066	-3.3748
C80	-8.4419	4.801	-3.5923
C81	-9.7707	5.1891	-3.2995
C82	-10.6533	4.2674	-2.7871
C83	3.3773	10.6508	4.0388
C84	3.0694	10.3577	5.3481
C85	2.5682	9.0788	5.6837
C86	2.3802	8.123	4.7083
H87	6.683	-3.2877	-0.5162
H88	3.1132	-1.786	-2.3755
H89	1.9618	-3.937	-1.922
H90	5.5229	-5.4535	-0.0606
H91	1.2762	-7.5971	-1.687
H92	-1.1273	-7.6851	-0.9885
H93	-0.3796	-4.6267	1.9323
H94	2.0072	-4.5322	1.2299
H95	6.4338	-0.233	-3.4471
H96	6.3036	-1.9923	-3.497

H97	-3.7508	-7.244	1.9371
H98	-2.3278	-8.1799	1.5001
H99	11.8019	-1.5695	-1.4041
H100	10.0576	-1.1375	0.3043
H101	7.6852	-0.9424	-0.3567
H102	-3.6482	-5.5617	3.7252
H103	-2.8711	-5.0742	6.0292
H104	-0.8847	-6.2461	6.943
H105	-7.2691	2.1357	0.1194
H106	-3.9617	1.5071	-2.5465
H107	-2.8715	3.5753	-1.6959
H108	-6.1666	4.2129	0.9832
H109	-2.5563	3.1808	1.4368
H110	-0.1398	3.2443	1.9986
H111	0.172	7.1693	0.2802
H112	-2.2613	7.104	-0.2859
H113	-6.6262	1.2587	-3.6615
H114	-7.2359	-0.3701	-3.3988
H115	1.0435	6.1629	3.264
H116	2.6798	5.5022	3.259
H117	-12.1817	2.2995	-1.7855
H118	-11.4817	-0.0459	-1.3813
H119	-9.1749	-0.7654	-1.9381
H120	2.7203	7.0256	0.2106
H121	3.6134	9.2589	-0.353
H122	3.9183	10.9686	1.4172
H123	7.6839	-1.5321	-5.1627
H124	9.428	-1.9396	-6.8217
H125	11.8153	-2.1483	-6.1314
H126	12.4304	-1.9362	-3.743
H127	0.9263	-7.8483	6.6843
H128	2.1744	-9.4942	5.3181
H129	1.4476	-9.9653	2.9784
H130	-0.4774	-8.8249	2.0186
H131	-6.9944	3.2476	-3.5902
H132	-7.7424	5.5322	-3.9882
H133	-10.0875	6.2132	-3.4769
H134	-11.6759	4.554	-2.5528
H135	3.7676	11.6298	3.7708
H136	3.2124	11.1037	6.125
H137	2.3312	8.8477	6.7187
H138	2.0021	7.1475	4.9966
Zn139	-4.7999	-3.1423	-0.3846
Zn140	4.1095	2.3621	-0.1106

Table S11 Coordinates for optimized geometry of binuclear Cd^{II}dithiocarbamate complex **6**.

Atom	**Coordinates (Angstroms)**		
Type	**X**	**Y**	**Z**
C1	-3.5615	-5.0663	-1.282
C2	-3.7424	-3.7921	-0.7297
C3	-2.8221	-2.7859	-1.0403
C4	-1.7618	-3.028	-1.9068
C5	-1.5622	-4.3142	-2.4204
C6	-2.4704	-5.3302	-2.1083
O7	-0.5369	-4.6725	-3.2715
C8	0.5561	-3.864	-3.5051
C9	1.0556	-3.862	-4.8098
C10	2.1528	-3.0634	-5.131
C11	2.7359	-2.2465	-4.1594
C12	2.2624	-2.2904	-2.8455

C13	1.1992	-3.1211	-2.5076
N14	-4.7916	-3.5622	0.238
N15	3.7377	-1.2803	-4.5513
C16	-4.8925	-4.5697	1.3156
C17	-6.0104	-5.5877	1.1472
C18	3.1916	-0.1056	-5.301
C19	2.3975	0.8354	-4.4055
C20	-5.5507	-2.4347	0.2724
C21	5.0099	-1.3319	-4.096
S22	-6.5011	-2.0778	1.6962
S23	-5.5885	-1.3436	-1.0844
S24	5.4837	-2.6121	-3.0114
S25	6.1782	-0.1154	-4.5663
C26	-6.1478	-6.6194	2.1348
C27	-7.1951	-7.5889	1.9846
C28	-8.0715	-7.5032	0.8689
C29	-7.9198	-6.5033	-0.0599
C30	-6.8856	-5.5459	0.082
C31	3.1038	1.749	-3.6407
C32	2.4541	2.6362	-2.7531
C33	1.0841	2.6086	-2.6338
C34	0.3092	1.7012	-3.4035
C35	0.964	0.7987	-4.313
C36	3.8721	1.4345	0.984
C37	4.9076	1.3691	1.9225
C38	4.8101	2.1354	3.0905
C39	3.6894	2.9303	3.3214
C40	2.6631	2.9956	2.3745
C41	2.7741	2.2657	1.1856
O42	1.6329	3.8579	2.6814
C43	0.351	3.766	2.1881
C44	-0.415	4.9298	2.3122
C45	-1.745	4.9453	1.8998
C46	-2.3235	3.8046	1.3294
C47	-1.5472	2.649	1.1945
C48	-0.2313	2.6127	1.6492
N49	6.0065	0.4445	1.7555
N50	-3.6658	3.8634	0.7957
C51	6.28	-0.4337	2.9131
C52	7.4607	-0.0176	3.7777
C53	-3.9431	5.0008	-0.107
C54	-4.6822	6.1699	0.5289
C55	6.673	0.2733	0.582
C56	-4.5998	2.898	1.0095
S57	7.7191	-1.1145	0.3791
S58	6.497	1.4159	-0.715
S59	-4.3449	1.6713	2.2136
S60	-6.0735	2.906	0.0683
C61	7.766	-0.8018	4.9396
C62	8.8741	-0.4156	5.7656
C63	9.643	0.7269	5.4139
C64	9.3311	1.4577	4.294
C65	8.2367	1.0823	3.4769
C66	-5.1285	6.1314	1.8332
C67	-5.8119	7.2292	2.4111
C68	-6.0447	8.3656	1.6762
C69	-5.6068	8.453	0.3269
C70	-4.9178	7.3418	-0.2647
C71	-5.2894	-6.7298	3.2643
C72	-5.4527	-7.7382	4.19
C73	-6.4845	-8.6927	4.0365
C74	-7.3347	-8.6151	2.9565

C75	-1.1073	1.6708	-3.2841
C76	-1.8664	0.7984	-4.0291
C77	-1.2302	-0.0817	-4.9362
C78	0.1408	-0.0799	-5.0736
C79	7.0184	-1.9524	5.3165
C80	7.3432	-2.6782	6.4427
C81	8.4344	-2.2925	7.2549
C82	9.1806	-1.1852	6.9193
C83	-5.838	9.6191	-0.4504
C84	-5.415	9.6979	-1.7581
C85	-4.74	8.6037	-2.3467
C86	-4.4984	7.4577	-1.6195
H87	-4.2671	-5.8602	-1.0597
H88	-2.9349	-1.7965	-0.6174
H89	-1.1002	-2.2126	-2.1681
H90	-2.3174	-6.3199	-2.526
H91	0.5703	-4.477	-5.5605
H92	2.5398	-3.0557	-6.146
H93	2.7315	-1.6775	-2.0852
H94	0.857	-3.1682	-1.4808
H95	-3.9243	-5.0765	1.3548
H96	-5.0182	-4.0304	2.2599
H97	4.0406	0.4194	-5.7361
H98	2.5897	-0.499	-6.1212
H99	-8.863	-8.2415	0.7662
H100	-8.5917	-6.4355	-0.9108
H101	-6.79	-4.7639	-0.6647
H102	4.1859	1.7801	-3.7217
H103	3.0466	3.3368	-2.1717
H104	0.5718	3.286	-1.9541
H105	3.9236	0.8504	0.0747
H106	5.6053	2.106	3.828
H107	3.6023	3.5157	4.2308
H108	2.0202	2.3325	0.4118
H109	0.0416	5.8131	2.7464
H110	-2.3308	5.8508	2.0176
H111	-1.974	1.7586	0.7506
H112	0.324	1.6866	1.5803
H113	5.364	-0.4507	3.5102
H114	6.4385	-1.446	2.5276
H115	-2.9735	5.3335	-0.4883
H116	-4.5148	4.6167	-0.958
H117	10.4815	1.0093	6.0459
H118	9.921	2.3286	4.0227
H119	8.0143	1.6745	2.5948
H120	-4.9593	5.244	2.4346
H121	-6.1502	7.1603	3.4411
H122	-6.5676	9.2127	2.1134
H123	-4.4916	-6.0085	3.4104
H124	-4.7852	-7.7994	5.0452
H125	-6.6041	-9.4831	4.7724
H126	-8.1328	-9.3431	2.8308
H127	-1.5814	2.3558	-2.5848
H128	-2.9475	0.7816	-3.9253
H129	-1.8294	-0.7679	-5.5281
H130	0.5936	-0.7781	-5.7673
H131	6.1785	-2.2754	4.7095
H132	6.7578	-3.5545	6.7077
H133	8.6814	-2.872	8.1401
H134	10.023	-0.8816	7.5364
H135	-6.3606	10.454	0.0106
H136	-5.5995	10.5963	-2.3406

H137	-4.411	8.6666	-3.3804
H138	-3.9833	6.6314	-2.0988
Cd139	-6.1877	0.386	0.8186
Cd140	7.1196	-0.7234	-2.1622

2. Molecular Electrostatic Potential (MESP)

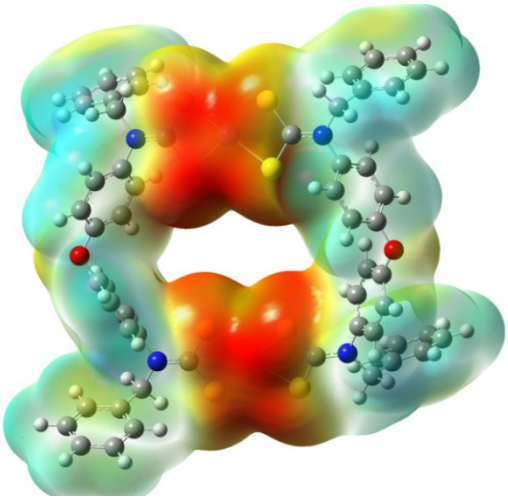

(a)

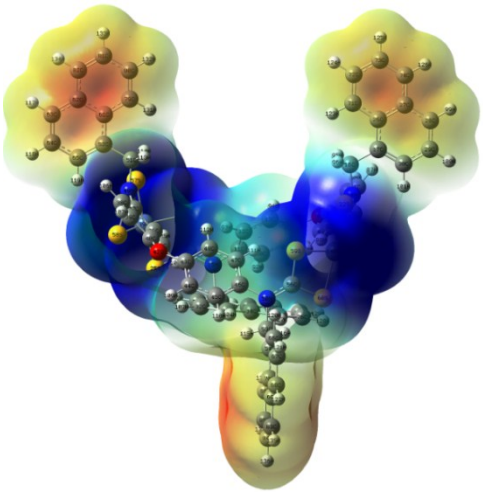

(d)

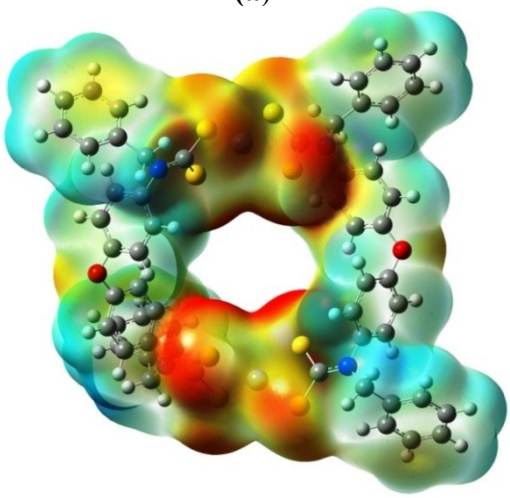

(b)

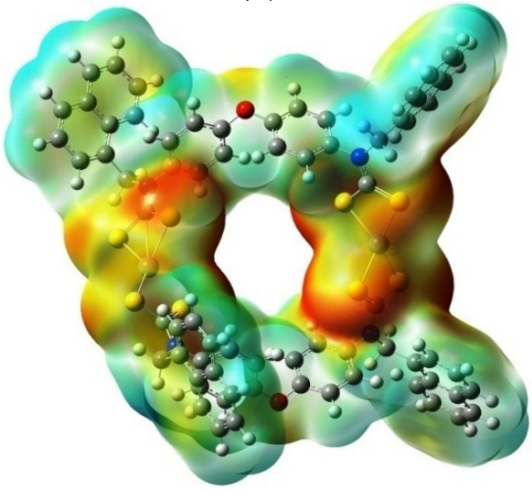

(e)

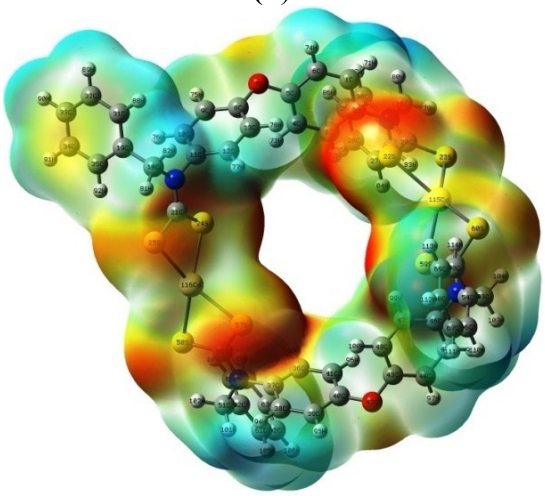

(c)

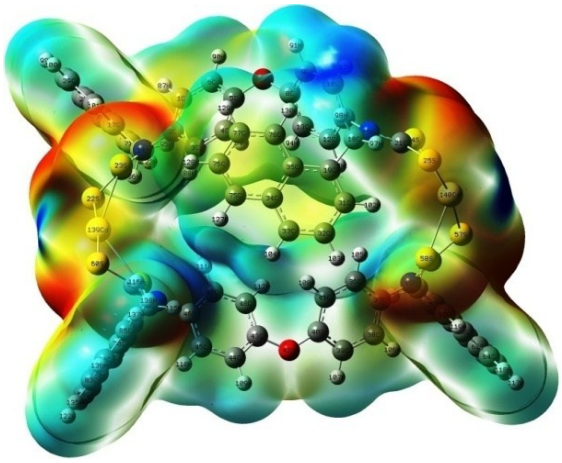

(f)

Fig. S32 Graphical representation of electron density from total SCF density (isoval= 0.0004; mapped with ESP, Red and blue colour represents localization of negative and positive potential respectively) for compounds **1** (a); **2** (b); **3** (c); **4** (d); **5** (e) and **6** (f).

3. Frontier Molecular Orbitals Analysis

For ligand precursors $\mathbf{L^1}$-$\mathbf{L^2}$, π-system of phenyl rings adjacent to ethereal oxygen contribute for HOMO, while LUMO is predominantly located on one of peripheral aromatic substituents. The HOMO and LUMO for **1** is localized over the various N-benzyl substituents whereas for complex **2** and **3**, the HOMO is predominantly delocalized over π-orbitals of one of the ligand framework excluding N-substituents, whereas coordinated dithiocarbamate moieties largely contributed for LUMO. However, in compound **4** all four 1-naphthylmethyl moieties are equally contributing to the HOMO whereas LUMO is delocalized over π-orbitals of ethereal phenyl rings and one of the coordinated dithiocarbamate functionality along with 1-naphthylmethyl moiety which is oriented towards side of the bowl shaped molecular framework. For complex **5**, HOMO is situated over nearly the whole molecule and LUMO is mainly localized at the only one of the 1-naphthylmethyl group connected to dithiocarbamate moiety; but for complex **6**, HOMO is delocalized over molecular fragment except 1-naphthylmethyl moieties and LUMO is mainly located around one of the cadmium centre. Furthermore, it appeared that HOMO-LUMO energy differences for the Ni^{II}dithiocarbamates **1** (3.6774 eV) and **4** (3.4649 eV) are significantly lower compared to their Zn^{II} and Cd^{II} analogues. Expectedly, the significant decrease in the HOMO-LUMO energy gap for compounds **1-3** compared to their ligand precursor $\mathbf{L^1}$ (4.5814 eV) is observed probably due to rigidity and extended conjugation conferred by coordinated dithiocarbamate ligand in molecular framework. The bulky 1-naphthylmethyl substituents lead to distortion in the molecular architecture affecting the conjugation could be the reason for increased HOMO-LUMO energy gap for compounds **5-6** compared to $\mathbf{L^2}$. The study depicted that extended conjugation decreases the HOMO-LUMO energy gap as it get remarkably decrease after variation of 1-naphthyl moiety instead of phenyl ring. Interestingly, the HOMO–LUMO energy gap for bimetallic dithiocarbamate complexes **1-6** is found in range 3.4649-4.7118 eV; which reveals the possible semiconducting properties of these compounds. In actual fact, the HOMO–LUMO energy gaps obtained by computational investigation are significantly higher than the UV-visible transmittance results probably due to presence of extensive noncovalent interactions in solid state. Thus, it adds merits to increase the potential applicability of this class of compounds towards semiconducting materials.

To the other hand, the computational investigations could be authenticated by the comparable experimental results. The HOMO-LUMO gaps obtained by computational study are clearly supported by the experimental UV-visible absorption data showing the comparable λ_{max} values for complexes **1-6** respectively.

References:

1. E. A. Davis and N. F. Mott, *Phil. Mag*., 1970, 22, 903.

2. (a) M. H. Habibi and N.Talebian, *Acta Chim. Slov*., 2005, 52, 53. (b) J. Tauc, *Mater. Res.Bull.*, 1970, 5, 721.

3. (a) R. Sharma and N. K. Kaushik, *J. Therm. Anal Calorim.*, 2004, 78, 953. (b) B. F. Ali,W. S. A.-Akramawi, K. H. A.-Obaidi and A. H. A.-Karboli, *Thermochim. Acta*, 2004,419, 39.

4. A. A. Memon, M. Afzaal, M. A. Malik, C. Q. Nguyen, P. O'Brien and J. Raftery, *Dalton Trans*., 2006, 4499.

5. D. C. Onwudiwe and P. A. Ajibade, *Int. J. Mol. Sci*., 2011, 12,1964.